PREDICTING PERMAFROST PROBABILITY IN A VARIABLE BOREAL ENVIRONMENT UTILIZING A MULTIPLE LOGISTIC REGRESSION MODEL, WHATÌ, NT, CANADA

SEAMUS V. DALY
Bachelor of Science, University of Lethbridge, 2018

A thesis
submitted to the School of Graduate Studies
of the University of Lethbridge
in partial fulfilment of the
requirements of the degree

MASTERS OF SCIENCE

in

GEOGRAPHY

Department of Geography and Environment
University of Lethbridge
LETHBRIDGE, ALBERTA, CANADA

PREDICTING PERMAFROST PROBABILITY IN A VARIABLE BOREAL ENVIRONMENT UTILIZING A MULTIPLE LOGISTIC REGRESSION MODEL, WHATÌ, NT, CANADA

SEAMUS V. DALY

Date of Defense: November 24, 2020

Dr. Philip P. Bonnaventure Thesis Supervisor	Associate Professor	Ph.D.
Dr. Craig Coburn Thesis Examination Committee Member	Professor	Ph.D.
Dr. Matthew G. Letts Thesis Examination Committee Member	Professor	Ph.D.
Dr. Stefan W. Kienzle Chair, Thesis Examination Committee	Professor	Ph.D.

Abstract

For remote communities, access to permafrost information for hazard assessment is a considerable challenge. This study applies analytical methods illustrating a time- and cost-efficient method for conducting community-scale permafrost mapping in the community of Whatì, NT. A binary logistic regression model was created using a combination of field data, digital elevation model-derived variables and remotely sensed products. Independent variables included categorical inputs such as vegetation, topographic position index and elevation breaks. The dependent variable is sourced from 139 physical checks of permafrost presence/absence. Vegetation was shown to be the strongest predictor of permafrost. The model predicts 50.0 % of the vegetated area is underlain by permafrost with a model accuracy of 91.4 % and spatial agreement of 72.8 % when compared to ground-truth pits. Compared to existing permafrost products this value is on the lowest edge of Whatì's current classification (extensive discontinuous) illustrating there could be less permafrost than presumed.

Acknowledgments

I would like to use this section to acknowledge the help and support I received throughout my work on this thesis. I would like to thank my family in Alberta, who supported me and offered me much needed breaks from my thesis. As well as my parents who supported me from afar. I would also like to thank my committee for their guidance throughout this thesis.

To my fellow lab-mates: Oliver Kienzle, Kyle Bexte, Madeleine Garibaldi, Nick Noad, Nick Hassink and Scott Vegter. You have improved my graduate school experience, both as fellow graduate students and as friends. I would like to extend a special thanks to Kyle Bexte and Oliver Kienzle for the help they provided me in my studies but importantly the hikes, fishing trips, ski runs and coffee runs they took me on. I'd like to thank Aimee Yurris for support throughout the whole process, you provided a stable home life which allowed me to focus on my studies. I would like to extend a special thanks to my supervisor Dr. Philip Bonnaventure who among many things, supported me in perusing a project in my home territory of the Northwest Territories when a project in the Yukon would have been easier.

I would like to acknowledge the Tłı̨chǫ Traditional Territory on which this study took place and say a heartfelt Masì cho to the Community Government of Whatì and the generous people of Whatì, especially my field assistant Collin Simpson. I only hope that this collaborative project has been as beneficial to you as the experience of working in Whatì has been to me.

This project was generously supported by a CCPN grant, remote sensing data was provided by Will Kochtitzky, logistical support and equipment was provided by Dr. Steve Kokelj and the Northwest Territories Geological Survey.

Table of Contents

List of Figures

List of Tables

List of Equations

List of Abbreviations

ALD	Active layer depth
AV	All variables
BLRM	Binary logistic regression model
CB	Coniferous forest (burnt)
CC	Coniferous forest
DEM	Digital elevation model
DOI	Department of Infrastructure
ENR	Department of environment and natural resources
FEM	Finite element model
GNWT	Government of the Northwest Territories
GPS	Global positioning system
LiDAR	Light detection and ranging
LS	Lac grandin low subarctic ecozone
LSC	Low shrub, clearing
LSOM	Low shrub, organic matter
MAAT	Mean annual air temperature
MAGST	Mean annual ground surface temperature
MAGT	Mean annual ground temperature
MW	Mixed-wood forest
MWB	Mixed-wood forest (burnt)
NDVI	Normalized difference vegetation index
NIR	Near infrared
PB	Peat Plateau (burnt)
PISR	Potential incoming solar radiation
PP	Peat plateau
RADAR	Radio detection and ranging
TPI	Topographic position index
TTOP	Temperature at the top of the permafrost
VO	Vegetation only
WL	Wetlands

Chapter 1

Thesis Introduction

1.1 Introduction

Understanding permafrost distribution is imperative for populations inhabiting permafrost environments. Permafrost is the only one of the big three components of the cryosphere (permafrost, glacier and sea ice) that humans inhabit year-round (French & Williams, 1976). Often missing from permafrost modelling studies is consideration of the human element. This thesis represents an intersection of geography and understanding permafrost as an ecosystem service to the peoples and communities of the Canadian north. This is the result of a project in the community of Whatì NT, started by the local government with a call to the permafrost community to help residents deal with the challenges driven by infrastructure projects and climatic change.

Understanding the distribution of permafrost is a fundamental first step to understanding the impacts of climate change on permafrost in the discontinuous permafrost zone (Camill & Clark, 1998; Jorgenson et al., 2010) where the interlaced nature of the boreal ecosystems and prominent wetlands create incredibly heterogeneous landscapes (Jorgenson et al., 2013). For many communities in the southern reaches of permafrost distribution, changes in local permafrost is occurring with respect to climate as well as the very dynamics and structure of the communities themselves (Fedorov et al., 1998; Hovelsrud & Smit, 2010; Pastick et al., 2014).

These communities now find themselves with very practical questions with respect to both the distribution of permafrost, and the potential for permafrost related hazards and infrastructure uncertainty (Allard et al., 2012). These communities are in a state of change,

including increased access, population and development. Thus, there is a need to assess potential changes and give stakeholders the ability to make informed decisions concerning permafrost related issues. Simple methods of permafrost detection and modelling can be used to preempt and address issues related to permafrost thaw (Michalowski & Zhu, 2006; Smith & Riseborough, 2010; Way & Lewkowicz, 2016).

The scale and the representation of permafrost in existing map products can be an issue when applied at a local scale (Higgins & Garon-Labrecque, 2018; Jafarov et al., 2018; Pastick et al., 2014). Many common permafrost maps use national level maps derived from ground surface temperatures and broad classifications of substrate materials (Heginbottom et al., 1995) or remote sensing data such as land surface temperatures, wetness and climate reanalysis data (Obu et al., 2019). These maps created at a regional or national scale (> 1 km^2 resolution, spatial extent = nation, circumpolar north) struggle to account for the impact of local vegetation and community structure on permafrost distribution.

1.2 Objectives

The aims of this thesis were to model the spatial distribution of permafrost around the community of Whatì and assess the impact of a recent (2014) forest fire on permafrost distribution. Fieldwork and analytical processes are streamlined and cost-effective in order to create an easily repeatable process that can be used in similar communities. Improved knowledge of the distribution of permafrost will provide a valuable product that will be used by the community government of Whatì to inform future planning and sustainable development. The key objectives that will contribute to the project goals are:

1. Explore the relationship between permafrost and local environmental variables in order to map the distribution of permafrost in the study area.

2. Investigate the sensitivity of the local environment and permafrost to change.

1.3 Thesis Structure

This master's thesis consists of 3 chapters. The first provides a brief introduction, including thesis objectives before presenting a literature review that serves to provide context for this thesis in permafrost sciences, specifically dealing with environmental influences on permafrost as well as permafrost mapping. Chapter 2 consists of an academic paper which details the work undertaken during this thesis to address the objectives outlined in chapter 1. Chapter 3 deals with conclusions and discusses the potential for future work.

1.4 Literature Review

1.4.1 Introduction

Permafrost refers to Earth surface material that remains below 0 °C for two or more consecutive years (French & Williams, 1976). Permafrost is a unique component of the "big three" components of the cryosphere (sea ice and glaciers being the others) as it is the only one that people live on year-round (French, 2011).

As climate change is altering the environment at unprecedented rates, local knowledge of permafrost accumulated over generations is unable to keep up with these changes. This leaves gaps in the knowledge pertaining to the future of local permafrost and how it will affect the people who inhabit its environment (Ford et al., 2016; Hovelsrud & Smit, 2010; Krupnik & Jolly, 2002). The growing body of scientific knowledge on the subject should be used in collaboration with local knowledge to adequately assess the risk thawing permafrost poses to communities and the lives of northerners.

Permafrost is not only an important foundation for human activity (Crate et al., 2017), it is an important part of northern hydrology (Jorgenson et al., 2013) and plays an important role in carbon storage and the storage of other contaminants such as mercury (Cooper et al., 2017; MacDougall et al., 2012; Schuur et al., 2015).

To adapt to a changing permafrost environment, it is important to understand the complex climate-ecosystem interactions that influence permafrost. As permafrost is a measure of thermal state, climate is viewed as the primary influence on permafrost with Mean Annual Air Temperature (MAAT) being the most important variable. As such permafrost mapping on regional (small) scale is mainly based on climate indices (Heginbottom et al., 1995; Obu et al., 2019).

Commonly used permafrost zone designations such as continuous (90-100 % of terrain underlain by permafrost), extensive discontinuous (50-90 %), sporadic discontinuous (10-50 %) and isolated patches (0-10 %) show a generalized classification of permafrost following a latitudinal pattern (Heginbottom et al., 1995) (Figure 1.1) often modified only slightly by substrate or large water bodies (Heginbottom et al., 1995).

While climate is an important influencer on permafrost, there are additional more localized influences that are necessary to accurately model permafrost distribution (Fisher et al., 2016; Shur & Jorgenson, 2007). These localized variables can generate considerable variability in permafrost conditions and have greater influence than regional impacts such as climate in local (large) scale permafrost studies (Camill & Clark, 1998).

The incorporation of modelling techniques is imperative for studying permafrost as they allow researchers to model information about distribution, condition and controlling factors with minimal field data. Demand for permafrost studies aimed at assessing permafrost distribution,

vulnerability and hazards is increasing as the effects of climate change on these environments become more present.

1.4.2 Permafrost, Environment and Climate

The presence, absence and condition of permafrost are controlled by a variety of environmental and climatological factors. At local scales, the important controlling factors of permafrost distribution and thermal state include: snow cover (Bonnaventure et al., 2017; Goodrich, 1982; Karunaratne & Burn, 2003), vegetation (Fisher et al., 2016; Jorgenson et al., 2013; Shur & Jorgenson, 2007), elevation, aspect (Bonnaventure & Lewkowicz, 2008; Deluigi et al., 2017; Etzelmüller et al., 2006; Panda et al., 2010), as well as thermal conductivity of soil, wetness and surficial geology (Burn & Friele, 1989; Fisher et al., 2016; Klene et al., 2001).

1.4.2.1 Effect of Snow

Snow cover is an important local variable influencing permafrost because of its insulating properties (Goodrich 1982). Snow cover can be responsible for considerable local permafrost variability as it can vary greatly across landscapes with respect to both accumulation and density (Zhang, 2005). Wind acts as a mechanism for redistributing snow depositing it in topographic hollows, anthropogenic structures, or vegetated areas. These features capture snow causing greater accumulation resulting in a thicker snowpack (Jafarov et al., 2018; Yang & Woo, 1999; Zhang et al., 2001).

In the winter, the thermal gradient between the air (cold) and the ground (warm) is steep due to differences in temperature (Lunardini, 1978; Lunardini, 1981). Without the insulating properties of snow, this steep thermal gradient causes rapid overwinter cooling of the ground as heat travels from the subsurface towards the cold atmosphere (Bonnaventure et al., 2017;

Goodrich, 1982; Harris, 1981). Overwinter cooling leads to colder permafrost, and reduced summer thawing (Harris, 1981; Karunaratne & Burn, 2003).

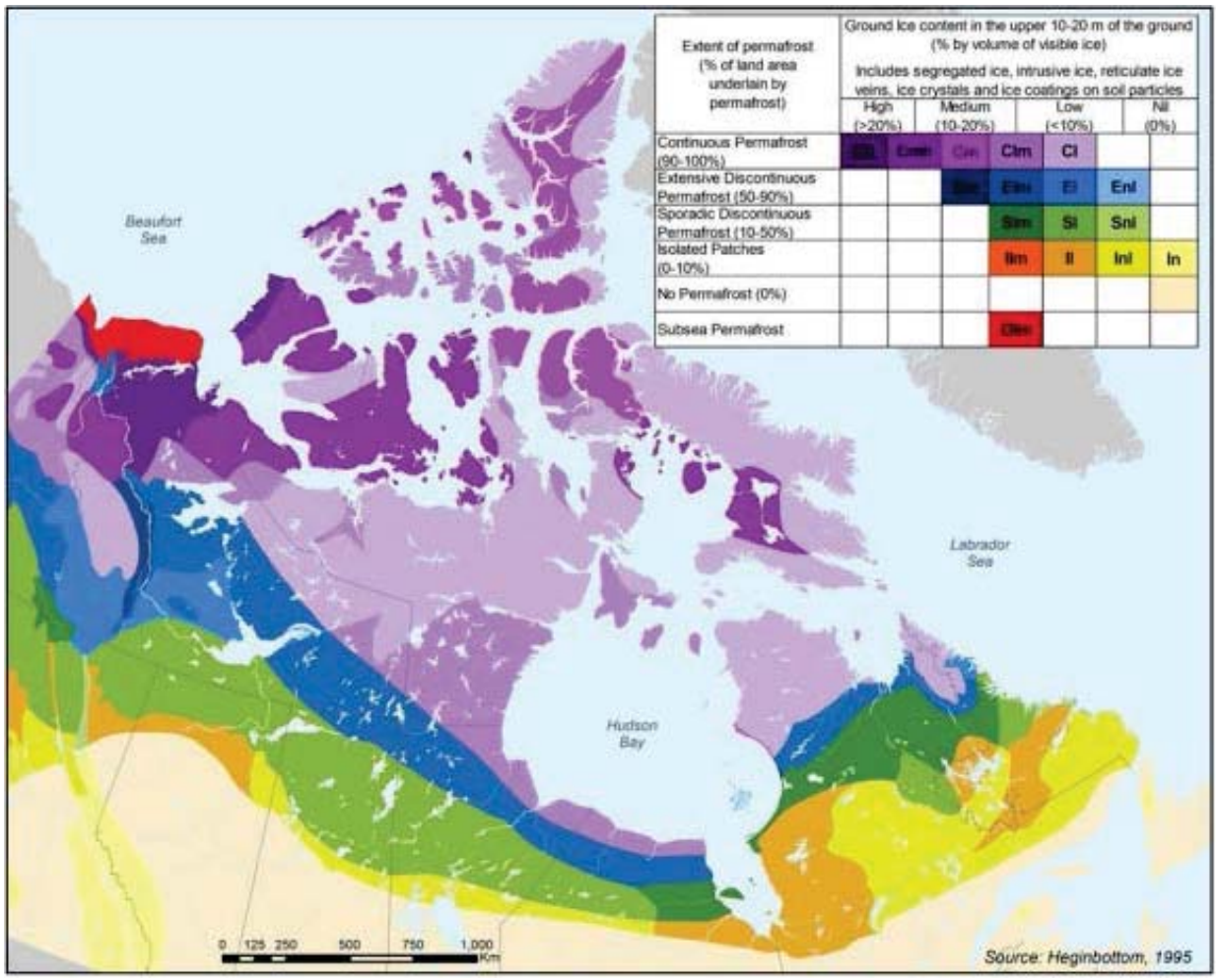

Figure 1.1 Permafrost map of Canada showing permafrost zones and ground ice content (Heginbottom et al., 1995). From National Atlas of Canada, 5th edition, Plate 2.1 (MCR 4177), Generated at scale 1:7,500,00

In permafrost environments, the active layer is a term used to define the portion of the ground above permafrost that freezes and thaws seasonally (Lachenbruch, 1994; Smith, 1990). The thickness of the active layer varies considerably across environments but is generally

shallower in areas with significant overwinter cooling (Bonnaventure & Lamoureux, 2013; Lachenbruch, 1994). The addition of snow to an environment prevents or slows down the rate of overwinter cooling, causing a net warming effect on the underlying permafrost (Bonnaventure et al., 2017; Garibaldi et al., 2020; Zhang et al., 2001). Figure 1.2 demonstrates that both maximum snow depth and the date at which it begins to build up determine whether permafrost will be present of absent.

1.4.2.2 Vegetation

At a local scale vegetation has a considerable effect on permafrost distribution. In Canada, the boreal forest overlaps with much of the discontinuous permafrost zone. The boreal ecosystem varies greatly over short distances (Fisher et al., 2016; Jorgenson et al., 2013), especially in lowlands where the boreal forest can be viewed as a patchwork of wetlands and fire disturbed areas (Camill & Clark, 1998).

Vegetation can have a variety of complex and often contradicting effects on permafrost attributes as the effects of vegetation change seasonally and within differing points of succession post disturbance (Smith & Riseborough, 2002; Smith et al., 2015). In the summer, tree canopies provide shade from incoming solar radiation, generating a cooling effect on permafrost (Brown, 1963; Fisher et al., 2016). In the winter, tree canopies can intercept snowfall preventing snow from reaching the ground (Brown, 1963; Fisher et al., 2016). Minimizing the insulating effect of the snow, increasing the connectivity between permafrost and the winter air causing a cooling effect (Brown, 1963; Fisher et al., 2016).

However, pre-climax ecosystem trees or shrubs typically result in the accumulation of snow as they block wind, creating a deposition zone where snow is deposited and not redistributed

(Bonnaventure et al., 2017; Brown, 1963). Vegetation can act as a mechanism of snow capture by providing structure for snow to adhere to causing increased snow buildup and increased winter insulation (Way & Lewkowicz, 2016, 2018).

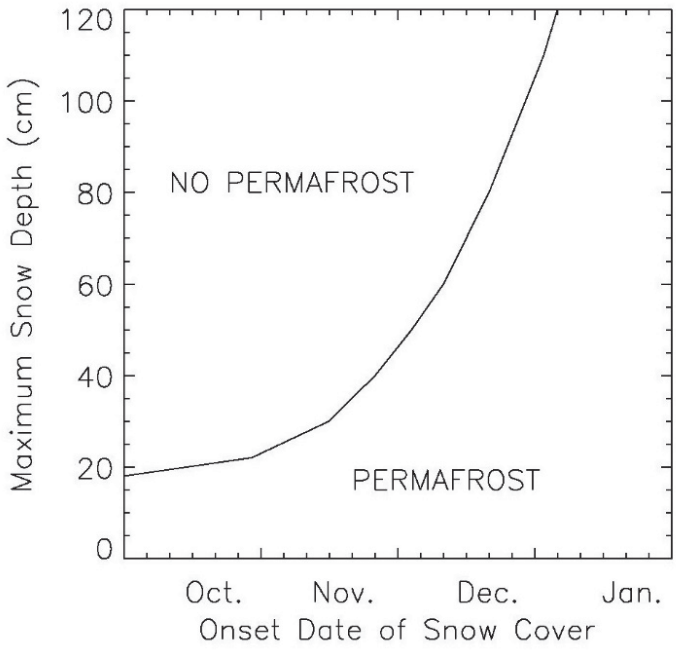

Figure 1.2 Results of simulation that shows presence or absence of permafrost in relation to snow cover onset dates and maximum snow depth. Annual amplitude of surface temperature is 20˚C (Zhang et al., 2001).

Additionally the evapotranspiration process leads to localized cooling due to chemical heat loss (Yi et al., 2007; Yoshikawa et al., 2002). Ground level vegetation including moss is able to retain moisture well, the effect of moss on permafrost in the winter is negligible, however in summer, moist or wet moss has a cooling effect as it has a low thermal conductivity creating a buffer between the summer air and permafrost (Porada et al., 2016).

1.4.2.3 Thermal Conductivity of Soil

Thermal conductivity of soils influence the rate at which heat enters or leaves the soil column (Hu et al., 2017). Thermal conductivity can vary seasonally as conductivity is related to soil moisture and the thermal conductivity of water changes seasonally (Hu et al., 2017; Zhuang et al., 2001). In a frozen state, the thermal conductivity of water is high, the opposite is the case in an un-frozen (Goodrich, 1982; Hu et al., 2017; Smith & Riseborough, 2002).

Figure 1.3 shows the results of soil calculations using three different soil conductivity equations (Farouki, Johansen, Luo), it demonstrates the differences between the equations as well as the calculated differences between frozen and unfrozen soil conductivity at different soil moisture contents. The conductivity of dry soil varies minimally from season to season, however moist soil will have a higher conductivity in the winter (frozen) and lower conductivity in the summer (un-frozen). This leads to a net cooling effect in moist soils as winter cooling takes place at a faster rate than summer warming. The effectiveness of climate driven ground temperature changes is altered by the effects of snow cover and vegetation which buffer the connectivity between air and ground temperatures (Klene et al., 2001).

1.4.2.4 Surficial Geology

The term surficial geology refers to unconsolidated sediments lying on top of bedrock. The effect surficial geology has on permafrost is due to two variables, thermal conductivity and soil particle size (Bonnaventure & Lewkowicz, 2012; Goodrich, 1982; Hu et al., 2017; Ling & Zhang, 2004).

The size of soil particles determines the level of drainage and distribution of moisture throughout the soil column (Painter et al., 2013; Van Vliet-Lanoë, 1985). Fine soils such as clay (Size < .002 mm) and silt (size between 0.002 and 0.05) often contain individual pockets of water, in permafrost these are referred to as segregated ice (Penner & Goodrich, 1982). Segregated ice

tends to grow through the process of cryosuction, where liquid water still present at temperatures below 0 °C migrates across the free-energy gradient and accumulates in lenses (Thomas et al., 2009). These fine grain soils are designated: frost susceptible. They tend to have higher amounts of segregated ice, a common component of terrain instability in permafrost environments, leading to frost heave and bedrock fracturing (Michalowski & Zhu, 2006; Thomas et al., 2009).

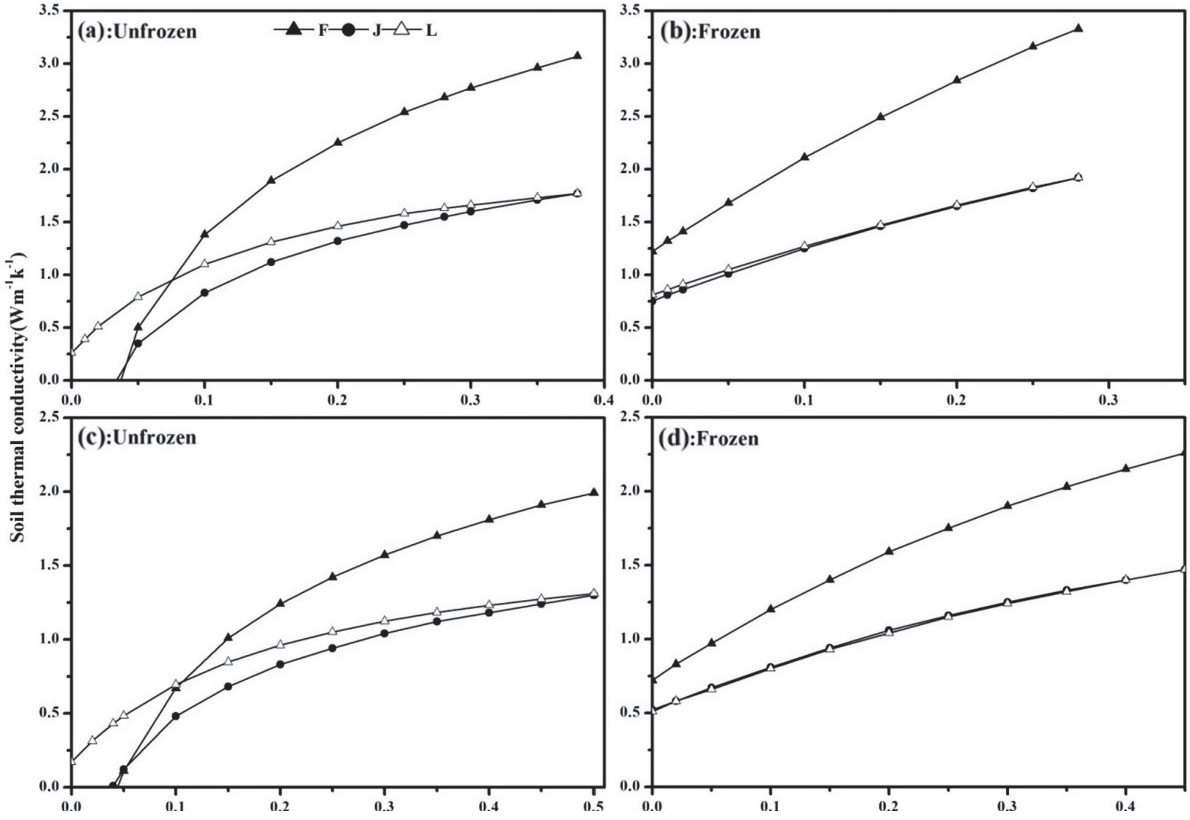

Figure 1.3 Comparison of thermal conductivity of Farouki, Johansen and Luo equations at two different sites TGL (a and b) and XDT (c and d) (Hu et al., 2017).

Coarser grain soils allow for a more even distribution of moisture throughout the soil column. This is less likely to cause major frost heave as the moisture is more evenly dispersed

throughout the soil column. This leads to more even freezing and more uniform thermal conductivity of the soil (Michalowski & Zhu, 2006).

Soil conductivity varies due to the presence of rocks and gravels. Course-grained mineral soils are often well drained, leading to drier soils. The minerals in the soils often have a higher thermal conductivity than a moist organic soil (Ling & Zhang, 2004; Thomas et al., 2009). This leads to minimal seasonal differences in thermal conductivity. While equal cooling and heating in the summer should minimize net heat gain or loss, the insulating properties of snow can greatly skew this towards annual net warming (Ling & Zhang, 2004; Romanovsky & Osterkamp, 1995) .

1.4.2.5 Elevation and Aspect

In mountainous environments elevation and aspect have a great influence on permafrost distribution. Higher elevations have lower air temperature compared to equivalent environments at lower elevations (Bonnaventure & Lewkowicz, 2008; Lewkowicz & Ednie, 2004). Mountain permafrost often occurs in mid- to high-latitude mountains and can occur at latitudes where permafrost is not present at sea level (Bonnaventure & Lewkowicz, 2008; Etzelmüller et al., 2001).

Aspect refers to the direction a topographic feature facing. The aspect of a feature changes the amount of solar radiation that is received by that feature. This can vary seasonally and at different latitudes. In mountainous environments the effect of aspect is exaggerated and can cause great differences in solar radiation received (Bonnaventure & Lewkowicz, 2008; Panda et al., 2010) In the northern hemisphere (0-90°) a southwest facing slope will receive more direct solar energy than a northeastern facing slope. This differential heating can lead to varying air and ground temperatures and causes permafrost to occur more commonly on north aspects (Panda et al., 2010).

1.4.3 Landscape Disturbances

Disturbances to the overlying ecosystem, including both vegetation and active layer can rapidly alter the combination of climatic and environmental controls influencing permafrost (Brown, 1963; Burn & Friele, 1989). Permafrost stability relies on an equilibrium between these influences, in the event of a terrain disturbance the post-disturbance conditions will vary compared to the pre-disturbance equilibrium (Burn & Friele, 1989; Smith & Riseborough, 2010).

Understanding the different types of landscape disturbances will shed light on the effect each one will have on underlying permafrost. Permafrost terrain disturbances can be divided into two general categories: natural and anthropogenic. Natural disturbances include: forest fires (Gibson et al., 2018; Holloway et al., 2020; Smith et al., 2015), thermokarst (French & Egginton, 1973; Regmi et al., 2012), mass wasting events (Kokelj et al., 2017; Luo et al., 2019), and vegetation succession (Burn & Friele, 1989; Shur & Jorgenson, 2007).

1.4.3.1 Forest Fires

Forest fires are a common natural disturbance on permafrost environments. Forest fire rates in the boreal forest are increasing in frequency and severity (Kasischke et al., 2010; X. Wang et al., 2015). Increased forest fire activity leads to more frequent changes in ecosystem related variables controlling permafrost presence. In areas where permafrost equilibrium is reliant on ecosystem, frequent alterations of these conditions will disrupt the equilibrium of permafrost and ultimately lead to less permafrost (Holloway et al., 2020; Smith et al., 2015).

The severity of the effects of forest fires on permafrost is dependent on burn severity and antecedent conditions (Holloway et al., 2020). Post-fire burn severity is affected by antecedent organic layer thickness, post-burn organic layer thickness, post-fire soil moisture content and the speed of vegetation succession. Revegetation to pre-fire conditions can take several decades,

however maximum active layer thickness is typically in the first 5 to 10 years post-burn (Yoshikawa et al., 2002).

Peatlands which contain a large amount of the permafrost in boreal study areas are more resilient to burn due to the high moisture content of the soils (Jafarov et al., 2013; Zhang et al., 2015) however, in cases of sever burn progressive thaw can continue to degrade permafrost in peatlands in the years following the burn, forming taliks, ultimately increasing the amount of unfrozen area in the peat plateau (Gibson et al., 2018).

1.4.3.2 Hydrological Disturbances

Hydrological disturbances can be either thermal or physical (Quinton et al., 2019). The specific heat capacity of water (4.184 Joules), a unit of measurement that represents the amount of energy required to change the temperature of a substance by one degree Celsius is relatively high. This property causes water to be more resistant to cooling (Ling & Zhang, 2004; Romanovsky & Osterkamp, 2000).

In the winter, water bodies are warmer than the air temperature (Wellman et al., 2013) and flowing water carries kinetic energy. This is shown in Figure 1.4, where a model is used to assess the thermal conditions of a soil column underneath a lake. In the spring when the active layer is thawing, water carrying thermal energy may trickle through deeper into the active layer all the way to the top of the permafrost causing faster spring thaw (Romanovsky & Osterkamp, 2000). These factors have a warming effect on the surrounding environment including adjacent permafrost (Wellman et al., 2013).

Flowing rivers can also cause physical disturbances by degrading and undercutting riverbanks (Shur & Jorgenson, 2007; Walker et al., 1987). This can cause instability in the bank and lead to mass wasting events that disturb the terrain and vegetation layers protecting underlying

permafrost or even completely expose permafrost to the elements (Burn & Lewkowicz, 1990; Kokelj et al., 2017).

Due to the net warming influence of water, lakes and rivers create taliks beneath them (Wellman et al., 2013). Taliks are discrete areas of unfrozen ground in permafrost zones. Beavers, and hydrological patterns due to dam construction have also been known to effect the condition of permafrost and permafrost features (Lewkowicz & Coultish, 2004).

1.4.3.3 Thermokarst

Thermokarst processes refer to thaw, erosion and subsidence that often occurs at or near the surface in ice rich permafrost terrain. A characteristic of thermokarst terrain is the occurrence of small thermokarst lakes which are often unstable and commonly drain causing new lakes to form and old lakes to dry up. (Côté & Burn, 2002; French, 2003; French & Egginton, 1973). These dynamic thermokarst environments are important to understand because of their capacity to alter local hydrology and vegetation cover.

Thermokarst lake drainage changes distinct local environments. The now dried lakebed will no longer have the damping influence of water, this will result in increased connectivity between adjacent permafrost and the environment. Any existing taliks will begin to degrade under these new climate-environment conditions.

The water from the collapsed thermokarst lake will either form a new lake or create a wetland, this has variety effects on the influences outlined in previous sections, altering vegetation, increasing soil moisture and developing taliks (Myers-Smith et al., 2008; Regmi et al., 2012).

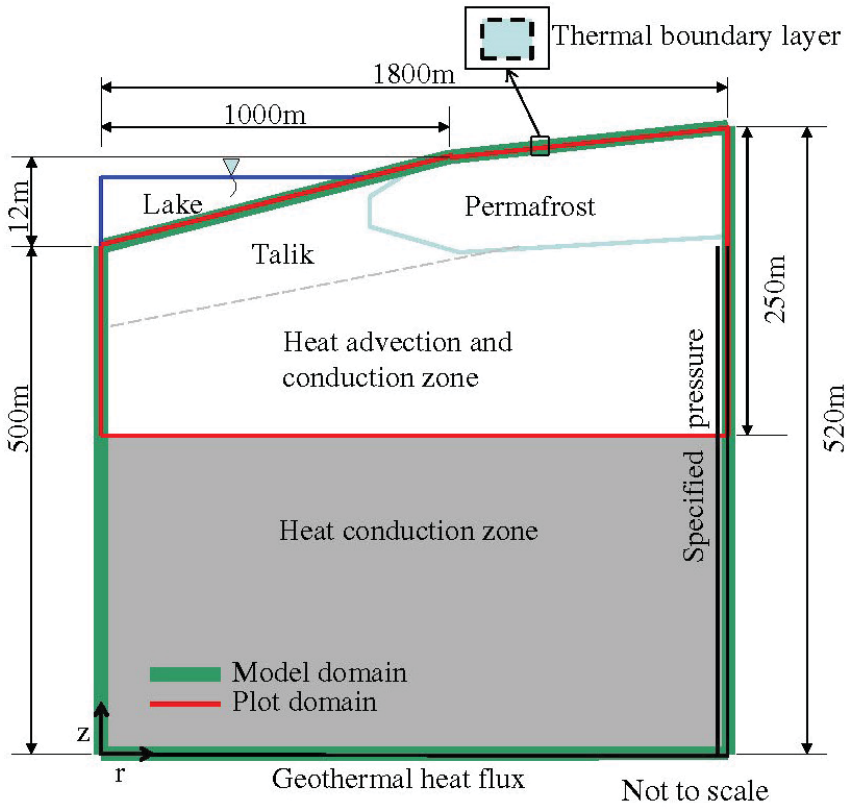

Figure 1.4 Cross section of two-dimensional cylindrical model. Boundary conditions are temperature, fluid pressure and heat flux. The thermal boundary layer is the boundary layer between ground and air or ground and lake (Wellman et al., 2013).

1.4.3.4 Mass Wasting Events

Mass wasting events refer to downslope debris movements (Luo et al., 2019). Common mass wasting events in permafrost terrain include solifluction, frost creep, active layer detachment slides and debris flows. Mass wasting events can range from small and slow solifluction and frost creep events to larger and more sudden events such as active layer detachments and debris flows (Lewkowicz, 2007; Mackay, 1970). Figure 1.5 provides examples of various slumps as well as associated secondar slides and debris dammed lakes.

Mass wasting events scour the landscape removing vegetation and the active layer. They can either completely expose the underlying permafrost or partially disturb the active layer and

overlying vegetation (Burn & Friele, 1989; Lewkowicz, 2007). Figure 1.6, A. shows the development of a slump. The destabilization caused by mass wasting events can cause a cascade of additional slides, either immediately or in the near future as a direct result of the initial destabilization on the underlying permafrost (Harris & Lewkowicz, 2000). While mass wasting events alter the environment, they are often incited by an initial destabilization caused by other disturbances.

1.4.3.5 Vegetation Succession

Vegetation succession refers to the natural change in vegetation over an area. Succession is typically slow moving and stops once it reaches a climax community. For the succession cycle to restart other disturbances are required. These disturbances include thermokarst action, mass wasting and forest fires.

Vegetation may grow on dried up lakes caused by thermokarst action. Slides and slumps may clear a large area of well-developed vegetation, eventually vegetation will begin to revegetate under most conditions (Burn & Friele, 1989). Vegetation succession post fire will determine if and when permafrost will return to per-burn conditions (Jafarov et al., 2013; Smith et al., 2015). Figure 1.6, B. illustrates the vegetation succession of an area cleared by a thaw slump. River movement and flooding may disturb or remove vegetation from lowland areas, restarting the cycle (Shur & Jorgenson, 2007). Vegetation removal and succession will alter the connectivity between underlying permafrost and the climate causing changes to the permafrost (Shur & Jorgenson, 2007), this can lead to either aggradation or degradation of permafrost (Fisher et al., 2016).

1.4.3.6 Anthropogenic Disturbance

The effects of anthropogenic disturbances typically resemble that of the effects of natural disturbances however the causes vary (Jin et al., 2008). Clearing a right-of-way for a pipeline, developing transportation infrastructure such as roads and train tracks and the construction of buildings changes the overlying ecosystem causing effects similar to that of a fire, or mass movement event. (Smith & Riseborough, 2010; Tarasenko et al., 2018).

Excavating the ground for a construction project will have similar effects to mass wasting events. It will clear vegetation and the active layer, increasing the connectivity between permafrost and the climate (Jin et al., 2008; Smith & Riseborough, 2010). Figure 1.7 illustrates different talik development scenarios under a right-of-way clearing.

Constructing a building will alter the equilibrium between climate and ground temperature. Buildings can introduce heat into an environment if not designed correctly. Cold climate engineering has introduced techniques to minimize the effects of buildings on underlying permafrost. These techniques include stilted buildings with room for convection, insulating fabrics applied directly to the ground and improved building insulation. (Brewer, 1958; Paramonov et al., 2016; Perreault & Shur, 2016).

1.4.4 Modelling in Earth Sciences

Models are simplifications of complex real-world processes; they are necessary as permafrost field data is typically recorded as point data. The collection of this data typically takes place in remote or difficult to access areas, so models are required to interpolate the data recorded by point data (Gruber & Hoelzle, 2001).

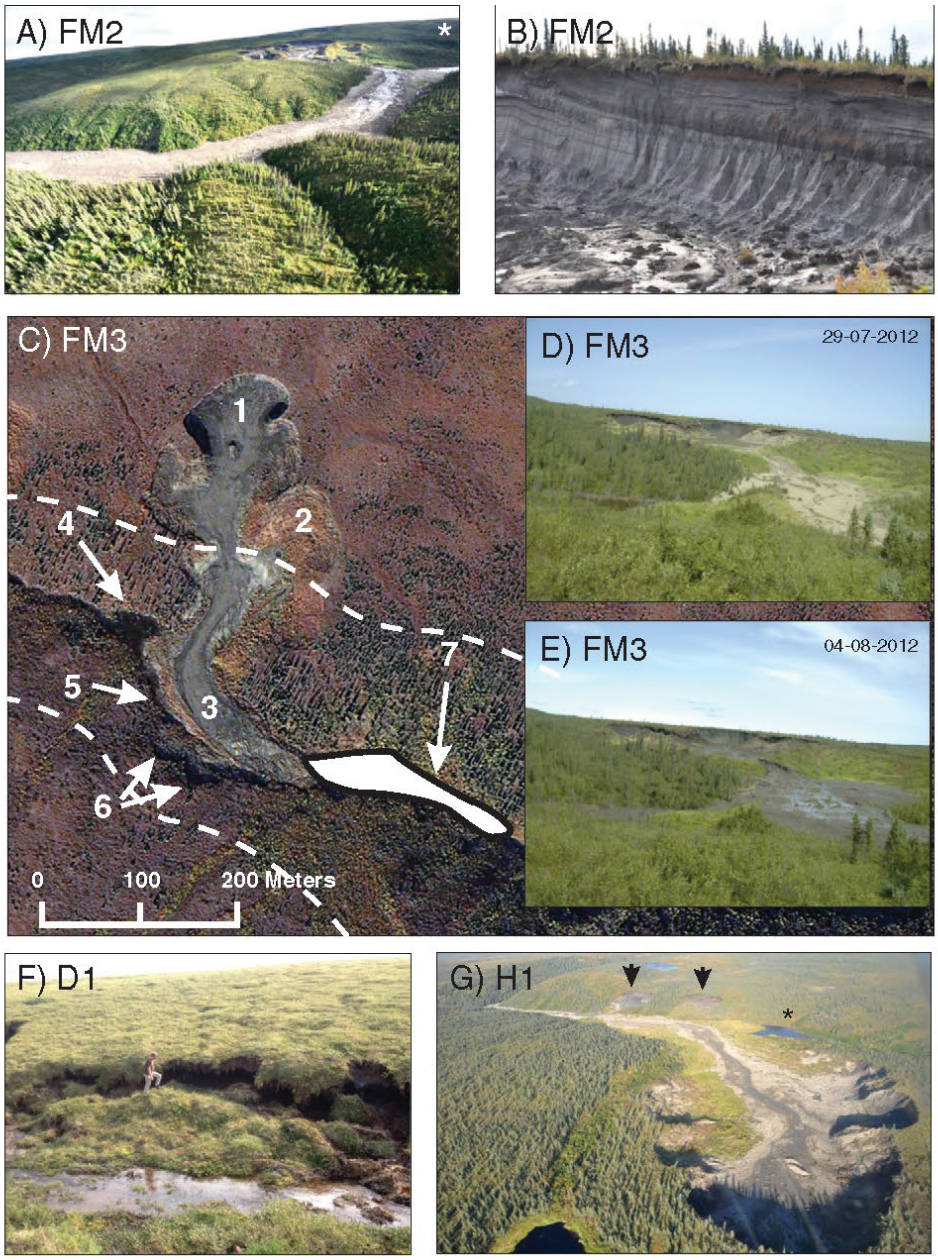

Figure 1.5 Examples of thaw slumps in the Peel Plateau. A) Slump FM2 and debris tongue, the Asterix indicates a debris dammed lake. B) Is the headwall of slump FM2. C) Image showing various slump features for slump FM3. D) Shows ablating slump headwall of FM3. E) Conditions during a mass flow event (FM3). F) Thermoerosion of slope. G) Secondary slumps indicated by arrows and debris dammed pond is indicated by the Asterix (H1) (Kokelj et al., 2015).

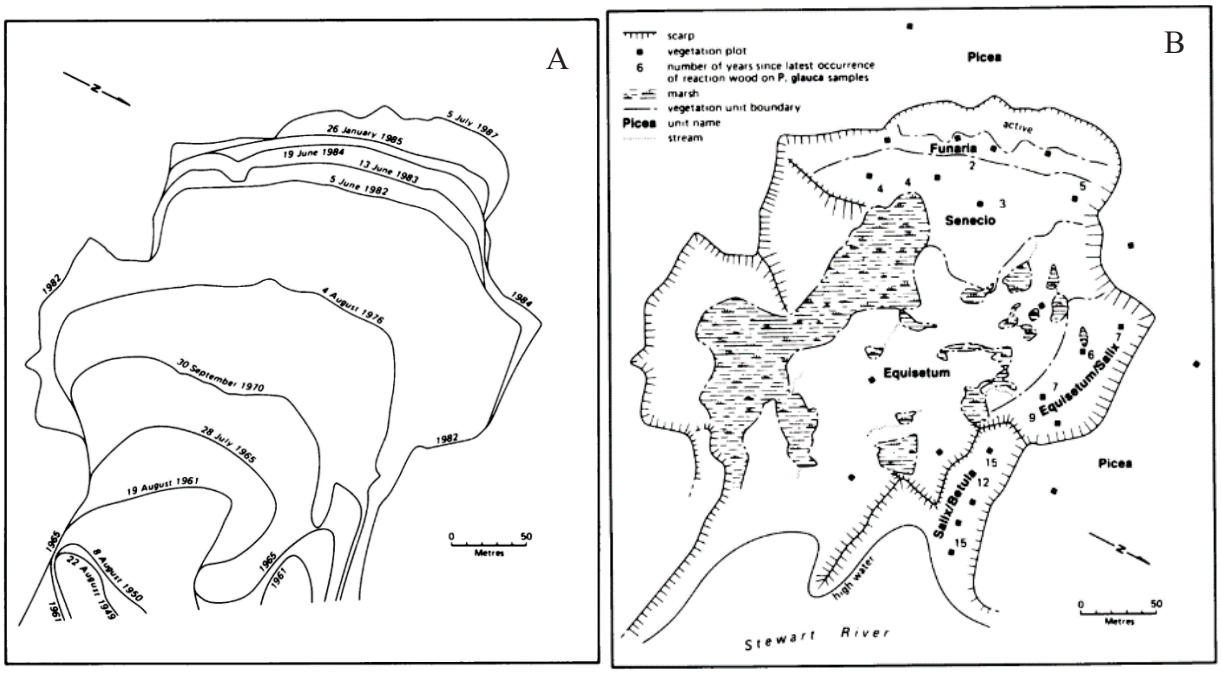

Figure 1.6 A) Shows the development of a slump near Mayo, YT from 1947-87. 2.6 B) Shows the vegetation succession measured in July 1987 (Burn & Friele, 1989).

Models in Earth science can be separated into two general classes based on scale, small-scale models, and large-scale models. Both types of model have different uses that are appropriate for their scale. Small scale models are used to study large areas or phenomena where the effects of local variables are negligible (Obu et al., 2019). These models are useful as they provide information of large areas that are difficult to instrument (Gruber & Hoelzle, 2001). While they typically generalize small-scale models are often necessary when working in remote and sparse locations.

Large-scale models can account for complex local influences and the interactions between them (Darrow & Jensen, 2016; Zheng et al., 2018), producing results that are spatially relevant at high resolutions. In permafrost studies these types of models are typically useful when conducting localized studies such as community-based permafrost research or environmental and

geotechnical engineering for development projects (Darrow & Jensen, 2016; Smith & Riseborough, 2010; Zhuang et al., 2001)

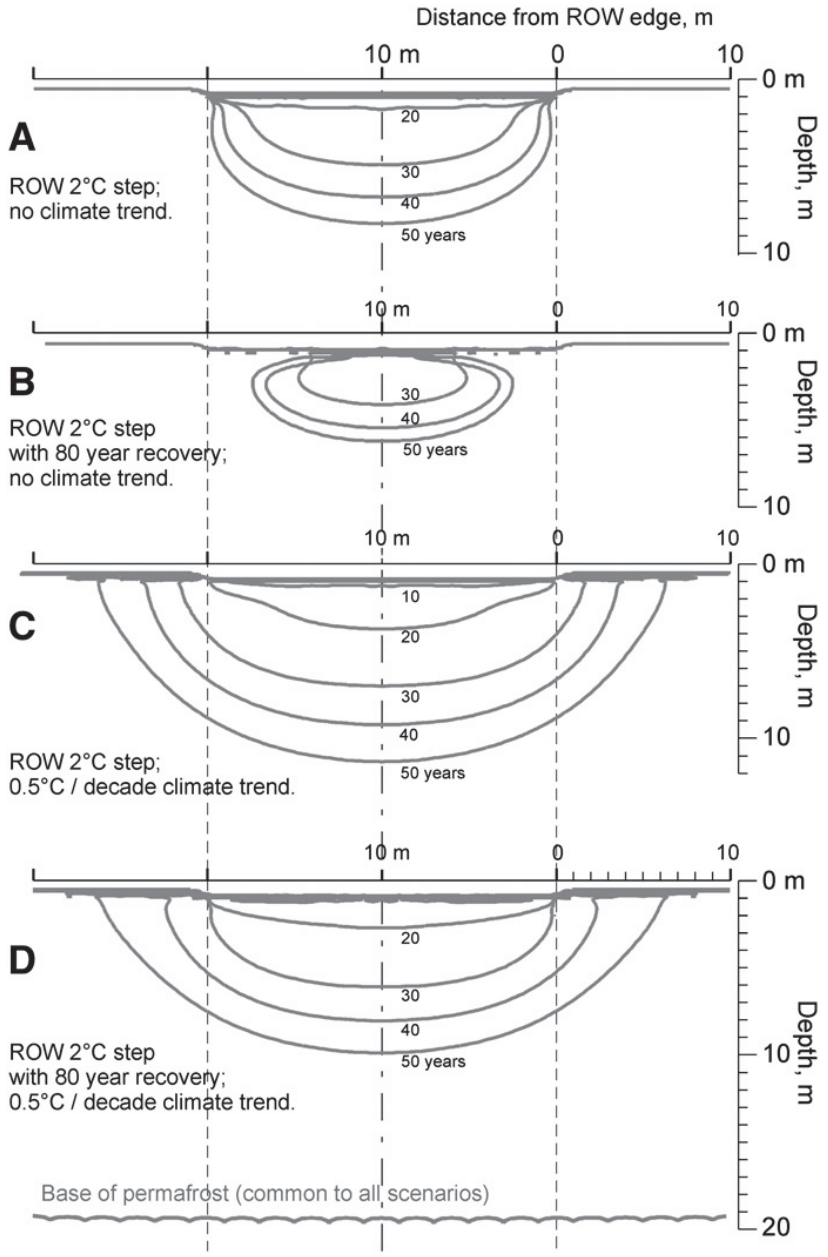

Figure 1.7 A variety of different talik development under right-of-way scenarios in Fort Simpson, NT. Scenarios vary in vegetation succession and climate warming (Smith & Riseborough, 2010).

Models are important in the field of permafrost studies, advancement of modelling techniques has contributed to a growing understanding of permafrost-environment-climate interactions (Goodrich, 1982; Hinzman et al., 1998; Taylor et al., 2013). This allows researchers to answer questions pertaining to permafrost conditions (Henry & Smith, 2001), distribution (Bonnaventure et al., 2012; Panda et al., 2010), energy balance (Ling & Zhang, 2004), stability (Fisher et al., 2020) and more.

Modelling techniques enable researchers to perturb current conditions for future climate scenarios in order to prepare for future permafrost conditions (Garibaldi et al., 2020; Riseborough et al., 2008; Taylor et al., 2013) and have increased the accessibility of permafrost research leading to an increased amount of research. Due to models being a simplification it is important to realize that models range in their ability to represent what you are modelling accurately. There are a variety of ways to validate models that are widely used.

The most obvious validation technique is to take measurements in the field. If you have actual recorded data of what you are modelling you are able to compare them, if your model agrees with your measured data then you can safely assume your model is valid (Panda et al., 2010).

Another common way to validate a model is to back-cast your model, meaning model things that have already happened and compare your back-casting results with actual measured record of what has happened (Oreskes et al., 1994; Riseborough et al., 2008). This practice is common for small-scale climate models however back-casting isn't as relevant for verifying large scale models that asses the interactions between permafrost and disturbances as they aim to assess changes after a disturbance.

A final method is to simply forecast your model and wait. Then compare measured record of what happens in the future to what your model has predicted would happen. The downside of

this method is that you must wait in order to validate your model. It is always important to validate models, otherwise there is no way to determine to what degree the model represents reality. Figure 1.8 shows the comparison between predicted model results and measured results this is an example of model validation. The next section will outline a few specific types of models as used in permafrost sciences.

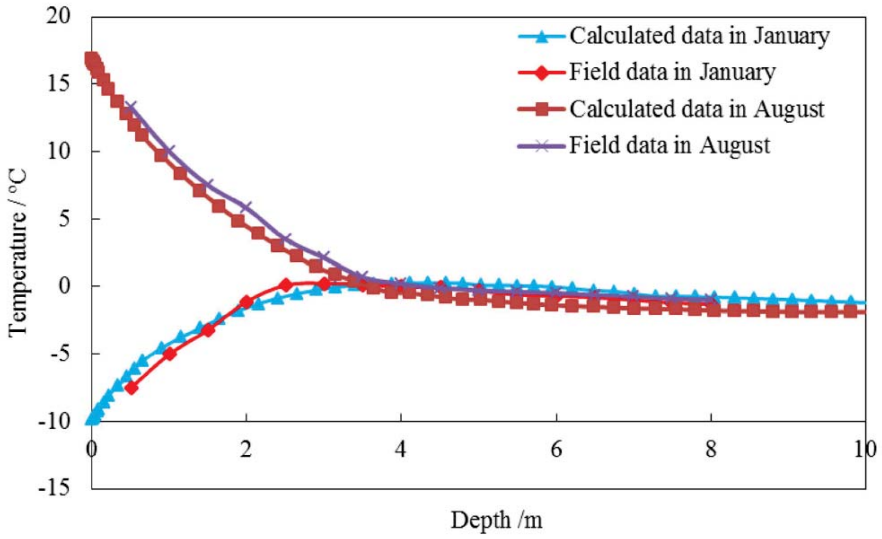

Figure 1.8 Comparison between predicted and measured temperature values (Ma et al., 2018).

1.4.4.1 Temperature at the Top of Permafrost (TTOP)

TTOP modelling is a method for determining the connectivity between climate and permafrost that is used in permafrost research (Wright et al., 2003). TTOP is useful to understand as it simplifies the different offsets which occur throughout a vertical section of air and ground. These offsets are important aspects of understanding and modelling the interaction between climate and permafrost (Romanovsky & Osterkamp, 1995; Smith & Riseborough, 1996). The four core terms that are key to understanding the TTOP model are lapse rate, surface offset, thermal offset and geothermal gradient (Henry & Smith, 2001; Smith & Riseborough, 2002).

The terms mentioned above represent differences between three points of measurement. These points are MAAT, Mean Annual Ground Surface Temperature (MAGST) and TTOP. Lapse rates are the change in temperature over a set elevation change. Lapse rates aren't the most important aspect of the TTOP model, however they cannot be ignored as lapse rates are an important controlling element of MAAT (Harris, 1981).

MAAT is an average temperature measurement taken at a standard height above the ground surface or snow surface. It is important to measure MAAT above the snow surface in order to ensure your measurements are not being influenced the insulating properties of the snowpack.

MAGST is the mean annual temperature measurement taken at the ground surface, it will be influenced by either vegetation of snow cover depending on the season. The difference in temperature caused by the warming and cooling effects of snow and vegetation is what leads to the 'surface offset'. This offset is simply the difference in temperature between MAAT and MAGST due to the influence of vegetation and snow. It can be either a warming or a cooling difference depending on the season however it is generally more important in the winter as permafrost climates are generally winter dominated.

TTOP is the temperature at the top of the permafrost. The thermal offset is the difference in temperature between TTOP and MAGST. The thicker the active layer is, the more disconnected the two temperatures will be. Different soil textures allow for more or less efficient transfers of heat which can also influence the temperatures and connection between TTOP and MAGST (Smith & Riseborough, 2002). Figure 1.9 shows a conceptual model of the TTOP equation.

The last of the core concepts; "geothermal gradient" is a natural ground temperature lapse rate. Deeper into the ground the temperature becomes less influenced by the above ground

temperature and at a certain point it begins to be influenced by a gradient of geothermal heat coming from deep beneath the surface.

The lower boundary of permafrost is established by extrapolating along the geothermal gradient from MAGST to 0˚C using a heat flux value. The value recorded in W/m^2 is determined by soil and geology characteristics (Goodrich, 1982; Wright et al., 2003). The geothermal gradient is mostly negligible unless the permafrost is deep or in an area high geothermal activity such as Iceland (Farbrot et al., 2007). TTOP is represented with this formula: TTOP = MAAT + Surface Offset + Thermal Offset (Henry & Smith, 2001; Smith & Riseborough, 2002). These factors can be calculated in a string of individual equations which eventually lead up to the TTOP equation. The TTOP equation is:

$$TTOP = \frac{(rk*nt*It)-(nf*if)}{P} \qquad (1.1)$$

The elements of the equation are as follows: *rk* is the result of the thermal conductivity ratio (*kt/kf*) where *kt* is the thermal conductivity of the ground in a thawed state and *kf* is the thermal conductivity of the ground in a frozen state. *Nt* and *nf* are scaling factors that describe the effect of vegetation and snow cover on the connectivity between MAAT and MAGST depending on the season. *It* and *If* are air thawing/freezing indexes calculated using thawing and freezing degree days (Celsius). *P* represents the annual period, therefore it equals 365 (days in a year) (Henry & Smith, 2001; Smith & Riseborough, 2002).

1.4.4.2 N-Factors

Nt and nf, two variables used in the TTOP equation outlined above are examples of n-factors. N-factors are functions used to transfer between MAAT and MAGST (Karunaratne

& Burn, 2003). N-factors range from 0.0 to 1.0. An n-factor of 0.0 represents a situation in which the air temperature has no effect on the underlying ground temperature (Karunaratne & Burn, 2003; Klene et al., 2001). This is not a realistic n-factor for permafrost environment. 1.0 reflects complete connectivity between ground surface and air temperatures.

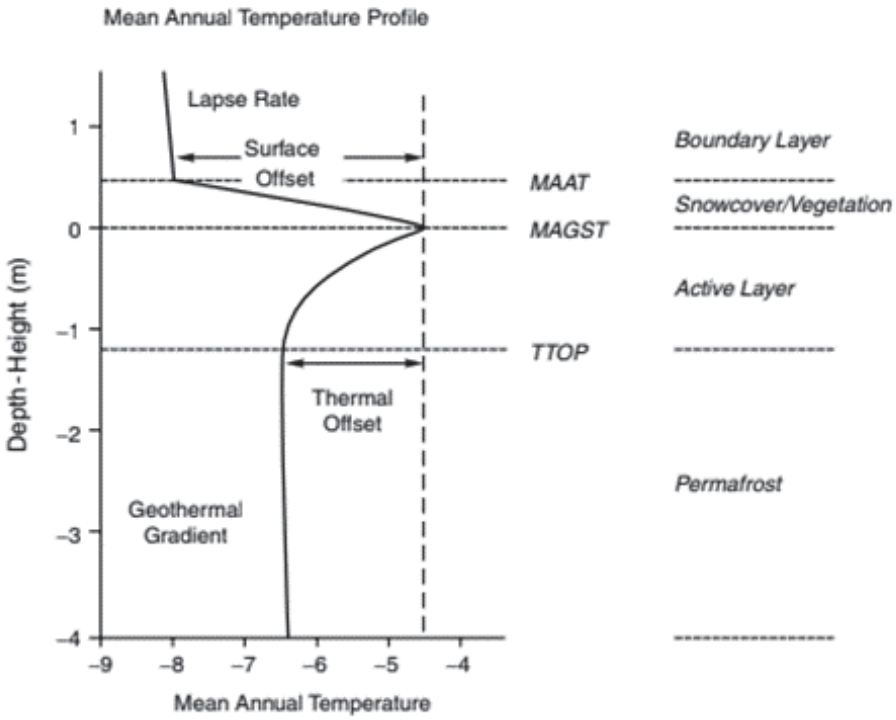

Figure 1.9 Mean annual temperature profile through the surface boundary layer (Smith & Riseborough, 2002).

N-factors vary depending on the season, due to varying thermal conductivity (frozen vs unfrozen), seasonal insulators such as snow and processes such as evapotranspiration which are responsible for diverse microclimates due to latent heat exchanges. Thus, they are classified as either freezing-n or thawing-n factors. N factors relate air to ground temperature, and are calculated by dividing freezing degree days (FDD) of soil over FDD of air for freezing n factors

or thawing degree days (TDD) of soil over TDD of air for thawing n factors (Lunardini, 1978). The equation for calculating n factors is shown below (Equation 1.2).

$$Nf = \frac{FDD_S}{FDD_A} \qquad Nt = \frac{TDD_S}{TDD_A} \qquad (1.2)$$

N-factors are functionally controlled be four variables: Snow cover, vegetation cover, soil type and standing water (Karunaratne & Burn, 2003). Figure 1.10 illustrates the n-factors of an area that is cleared of snow and an area that captures increased amounts of snow. The specifics of these variables are explained in earlier sections, n-factors aim to quantify the effect these variables have on the connection between the environment and permafrost in order to derive reasonable predictions of MAGST from MAAT throughout the year.

The temperature value of MAAT is also important, as seen in Figure 1.11 freezing n-factors are a function of both snow depth and MAAT. The magnitude of the temperature can cause the n-factor to increase. Looking at two different areas, both have the same snow depth but one has a MAAT of -2ºC and the other has a MAAT of -12ºC. The nf associated with the colder MAAT will be higher than the warmer MAAT. This is attributed to active layer thickness (Smith & Riseborough, 2002).

1.4.4.3 Shur and Jorgenson Classification

In their 2007 paper: *Patterns of Permafrost Formation and Degradation in Relation to Climate Ecosystems*, researchers Shur and Jorgenson outline a conceptual model that classifies permafrost formation by the climate and ecosystem in which it is found. Climate ranges from High Arctic to Cold Temperate and the ecosystem ranges from Late to early succession and from no

disturbances to very disturbed. The five types of permafrost outlined are “climate-driven”, “climate-driven, ecosystem modified”, “climate-driven, ecosystem protected”, “ecosystem driven” and ‘ecosystem protected’.

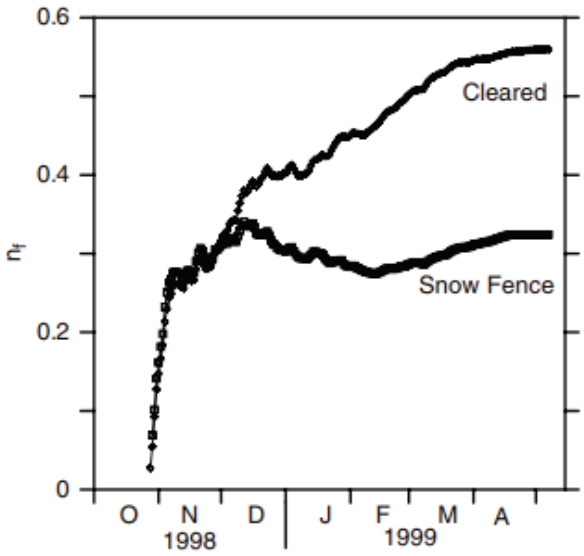

Figure 1.10 Daily cumulative n-factors at cleared and snow fence sites in the winter (Karunaratne & Burn, 2003).

The main benefit of this method of modelling is how easily it can be used to simplify complex climate-ecosystem controls on permafrost by placing it on the climate – disturbance graph shown in Figure 1.12. This makes comparison between different study areas simple and provides more information other simple products. The method is also easily scalable and can be applied to larger regions such as ecoregions or smaller regions such as municipalities.

1.4.4.4 Empirical Probability Models

Use of statistical-empirical models to model permafrost presence has become increasingly common in the field of permafrost science (Riseborough et al., 2008). Regression,

both linear and logistical have been shown to produce spatially relevant results when used to predict the probability of permafrost presence (Baral & Haq, 2020; Kremer et al., 2011). Logistic regression is often used as it allows for models incorporating both continuous and categorical variables (Panda et al., 2010).

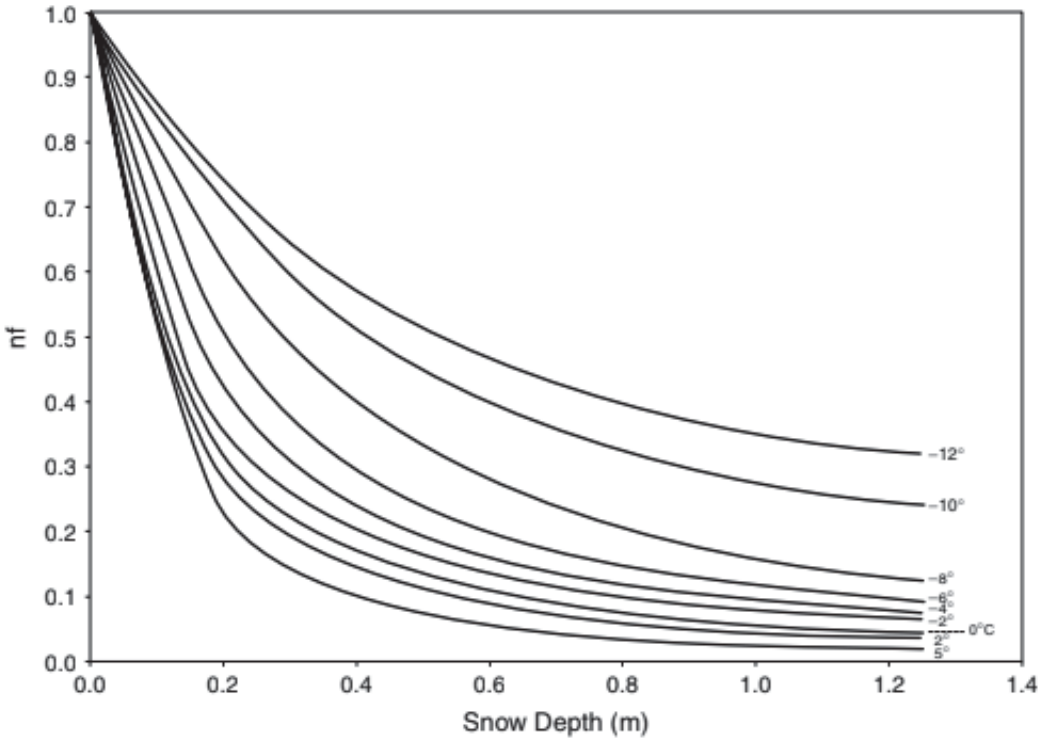

Figure 1.11 Freezing-n factor shows as a function of snow depth and Mean Annual Air Temperature (Smith & Riseborough, 2002).

1.4.4.4 Empirical Probability Models

Use of statistical-empirical models to model permafrost presence has become increasingly common in the field of permafrost science (Riseborough et al., 2008). Regression, both linear and logistical have been shown to produce spatially relevant results when used to predict the probability of permafrost presence (Baral & Haq, 2020; Kremer et al., 2011). Logistic

regression is often used as it allows for models incorporating both continuous and categorical variables (Panda et al., 2010).

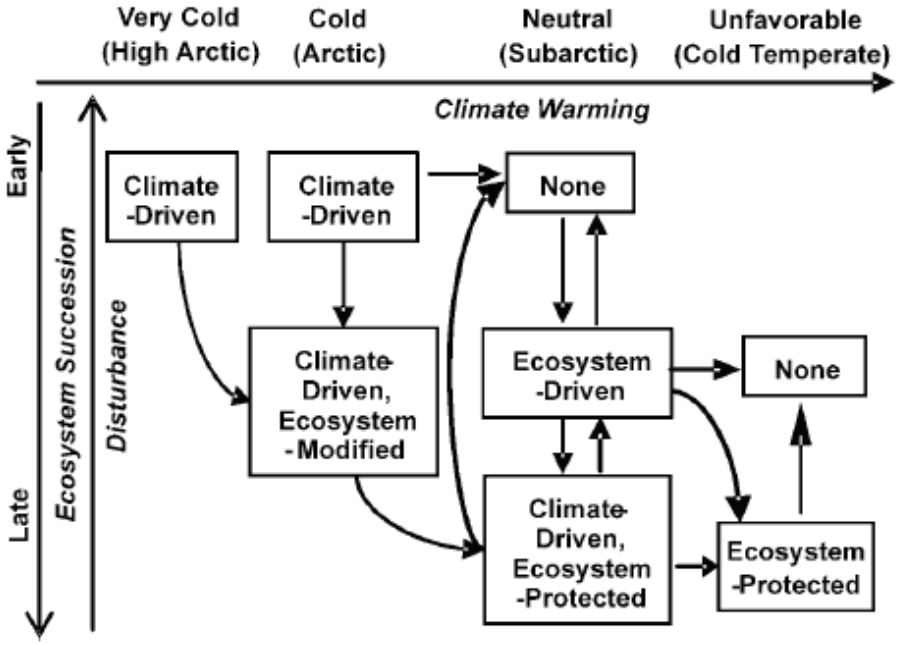

Figure 1.12 Permafrost conditions in relation to climate, ecological succession and disturbances (Shur & Jorgenson, 2007).

In addition to creating accurate probability maps, empirical models do not rely heavily on field data collection as model inputs can often be derived from remote sensing products such as Digital Terrain Models generated using synthetic aperture radar (SAR) or laser scanning, spectral image classification and airborne geophysics such as ground penetrating radar (Jorgenson & Grosse, 2016; Kääb, 2008), or data mined data sources such as meteorological data and topographic characteristics, (Zhao et al., 2012). Dependency on large amounts of field data is a large obstacle when conducting permafrost research in remote areas (Gruber & Hoelzle, 2001; Zhao et al., 2012). Empirical models are also useful as the modelling can be performed in easily accessible software such as statistical analysis software or GIS packages (Panda et al., 2010).

Machine learning techniques including random forest, support vector machines and neural networks have been used successfully to accurately model permafrost presence (Baral & Haq, 2020; Kremer et al., 2011). Regression models have shown to be transferable across regions assuming the variables controlling permafrost condition and presence remain the same (Bonnaventure & Lewkowicz, 2008; Lewkowicz & Bonnaventure, 2008). For example when modelling the presence of mountain permafrost Bonnaventure and Lewkowicz (2008) found that locations on similar ends of a scale that ranged from elevation controlled to solar radiation controlled could be modelled accurately using a model created in a different study area (Lewkowicz & Bonnaventure, 2008)

1.4.4.5 Finite Element Models (FEMs)

Numerical models are purely mathematics-based models, for this reason they are very easy to implement and compute if you have the appropriate hardware and a good understanding of the model at hand. Numerical models are used heavily in Geography because of their relative ease of use and powerful ability to model complex interactions. They are very flexible as the equations used can be edited and tweaked depending on your scenario and input.

Finite element models (FEMs) are a type of numerical model used by engineers and scientist to model physical processes and interactions. FEMs work by breaking complex physical interactions between a multitude of elements down into individual elements (finite elements) (GEO-SLOPE International, Ltd. 2014). finite elements are represented by constants, inputs and equations. Once they are isolated it is much simpler for them to be modified and applied to a specific problem. This final combination process is performed in FEM software. FEMs are often used to model interactions between permafrost and the effects of the construction of buildings and infrastructure. (Ma et al., 2018; Smith & Riseborough, 2010; Tarasenko et al., 2018) as these

interactions complex. Figure 1.13 shows a schematic created in TEMP/W as part of a FEM process. Another benefit of FEMs is the flexibility they provide the user with. Finite element models can be performed in a variety of different software. Finite element modelling in Earth sciences has progressed to a point where there are premade models for a wide range of processes.

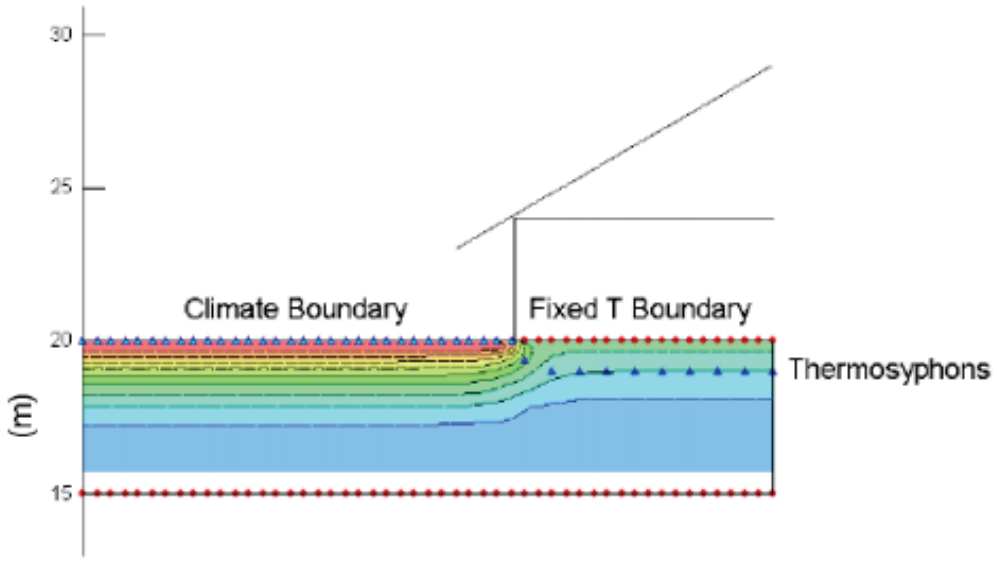

Figure 1.13 TEMP/W model of structure with thermosyphons underneath. (GEO-SLOPE International, Ltd. 2014).

Chapter 2

Thesis Paper

Predicting Permafrost Probability in a Variable Boreal Environment Utilizing a Multiple Logistic Regression Model, Whatì, NT, Canada

Submitted for review to the journal: Permafrost and Periglacial Processes on 07/08/2020

*Seamus V. Daly[1], Philip P. Bonnaventure[1] & Will Kochtitzky[2, 3]

[1]Bonnaventure Lab for Permafrost Science, Department of Geography and Environment, University of Lethbridge, Lethbridge, AB, Canada, T1K 3M4

[2]Department of Geography, Environment and Geomatics, University of Ottawa, Ottawa ON, Canada, K1N 6N5

[3]Climate Change Institute, University of Maine, Orono, ME, USA, 04469

*Corresponding Author email: seamus.daly@uleth.ca

Key words: Permafrost, Boreal, Empirical Statistical, Logistic Regression, Forest Fire

2.1 Abstract

For remote communities in the discontinuous permafrost zone, access to current permafrost distribution maps for hazard assessment is limited and the products are often inadequate for use in community planning. In this study, established analytical methods are applied to illustrate a time- and cost-efficient method for conducting community-scale permafrost mapping in the community of Whatì, NT.

A binary logistic regression model (BLRM) was created using a combination of field data (ground-truth pits), DEM-derived variables and remotely sensed products. Independent variables included vegetation, topographic position index (TPI) and elevation bands. The dependent variable is sourced from 139 physical checks of permafrost presence/absence sampled across a boreal environment in the extensive discontinuous permafrost zone.

Vegetation is the strongest predictor of permafrost in the model. The model predicts 50.0 % of the vegetated area is underlain by permafrost with a model accuracy of 91.4 %. Compared to existing permafrost products this value (50.0 %) is at the lowest range of Whatì's current classification (50-90 %). The model was perturbed to explore potential changes in the ecosystem brought on by forest fires, demonstrating that when coupled with predicted future climate change the permafrost area will likely continue to decrease. This model gives insight into the permafrost distribution around Whatì and will be used to inform future planning and development.

2.2 Introduction

Communities in permafrost regions face considerable uncertainties and challenges as climate warms and permafrost thaws (Hovelsrud & Smit, 2010). As permafrost is expected to thaw from the top down, near surface permafrost is considered the highest risk (Zhang et al., 2008). This is concerning with regards to the human environment that overlaps with areas underlain by permafrost as degradation of near surface permafrost will have the most notable effect on the overlying terrain. (Nelson, 2003).

Thawing permafrost is associated with considerable environmental challenges, including the releases of stored carbon (MacDougall et al., 2012; Schuur et al., 2015), release of toxins into the environment (e.g. mercury) (Schuster et al., 2018), ancient viruses and diseases (Legendre et al., 2015). Changes in hydrological regimes (Connon et al., 2014; Quinton et al., 2011), landscape instability and hazards associated with thermokarst which pose additional challenges. Thaw poses problems for both existing and future infrastructure including buildings, roads and pipelines (Bommer et al., 2010; Doré et al., 2016). These issues are further exacerbated by natural disturbances common in the boreal forest environment, especially forest fires which are presently occurring at a shorter recurrence interval over a longer season (Holloway & Lewkowicz, 2020).

Mapping the distribution of permafrost in the discontinuous permafrost zone of southern Northwest Territories, Canada is challenging. Although the terrain is relatively flat without major topographic relief, the landscape is heterogeneous with complex interactions between the boreal ecology and prominent wetlands (Jorgenson et al., 2013). For some communities in the

southern reaches of permafrost zones, changes are not only occurring with respect to climate but also with respect to the dynamics and structure of the built human communities themselves. As a result, these communities are concerned with the distribution of permafrost, permafrost related hazards and infrastructure uncertainty. As these communities change and grow, there is a need for simple methods of permafrost detection and modelling to give community stakeholders the ability to make better decisions with better maps.

Frequently, the scale and the representation of permafrost (e.g. continuity classes, TTOP) in existing products can be an issue at the community level. Many existing permafrost products have utilized national level maps derived from ground surface temperatures and broad classifications of substrate materials (Heginbottom et al., 1995) or remote sensing data (Obu et al., 2019) which cannot take into account small scale variations that impact permafrost distribution and community uses of the land.

The community of Whatì has a population of 470 people (2016) and is currently fly-in only during the summer and connected to a seasonal road network during the winter months (Jan. 28 – Apr. 15) (Government of the Northwest Territories, Department of Infrastructure [GNWT DOI], 2020). In 2022, construction of a road connecting the community to the all-season road network is to be completed. This road is expected to increase the population and demand for infrastructure and services, yet a permafrost distribution map is not currently available for this area to inform this development.

The objective of this study was to model the spatial distribution of permafrost in and around. This study demonstrates a rapid and cost-effective method for mapping permafrost,

generating a probability map that that will be used by the Community Government to inform development of existing and future infrastructure.

2.3 Study Area

The study area is defined by the 60 km^2 municipal boundary of Whatì, NT (Figure 2.1) and is divided into a northern and a southern section by a ridge running east to west (Figure 2.2). The built community of Whatì (elevation of 247 m asl) is situated in the far west of the study area against the shores of Lac La Martre. The study area has a relief of 44 m, ranging from 238 m asl to 282 m asl.

Whatì is classified as subarctic with cool summers and year-round precipitation according to the Köppen-Geiger climate index (Dfc) (Peel et al., 2007). The closest long-term weather station is located in Yellowknife, NT, 164 km to the southeast with a MAAT of -4.3 °C and an annual average precipitation of 288.6 mm over the 1981-2010 climatic normal (Government of Canada. 2020, September 17. Yellowknife A Northwest Territories. https:// climate.weather.gc.ca). Winter is the dominant season, as only 5 months have a mean daily average above 0 °C (May-September; Environment Canada, 2020). The annual average temperature in Yellowknife increased by 2.5 °C from 1943 to 2011 (Laing & Binyamin, 2013). Under the RCP4.5 climate scenario, Yellowknife's annual mean air temperature is projected to increase by 2.2 °C to -2.5 °C for the 2021-2050 time period compared to -4.7 °C for the 1976 to 2005 time period (The Prairie Climate Centre. *Climate Atlas of Canada* [Version 2, July 10, 2019]. https:climateatlas.ca).

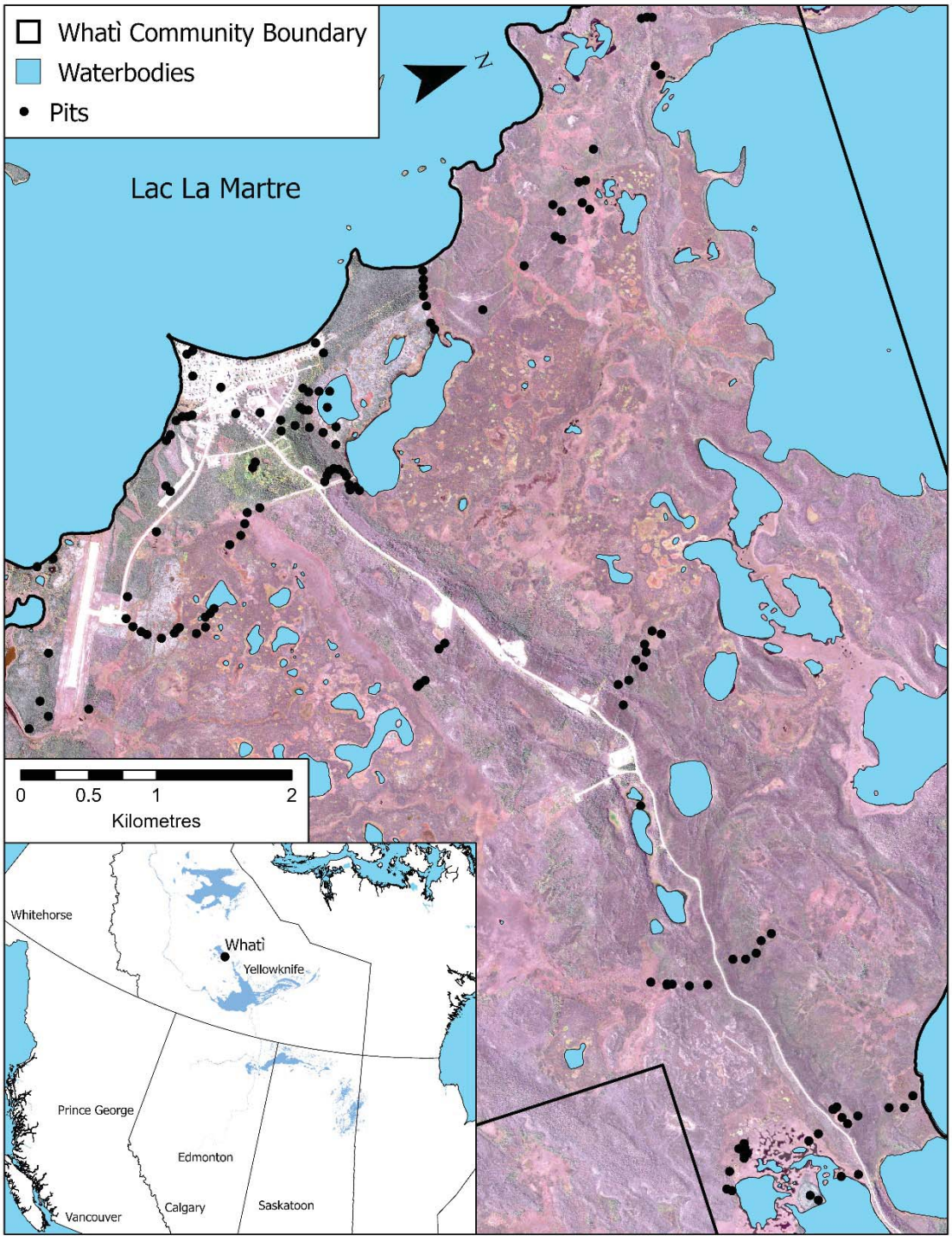

Figure 2.1 Study area extent in and around the community of Whatì as well as the location of ground-truth pits (pits) recorded in the field (139). Imagery © [2017] DigitalGlobe, Inc.).

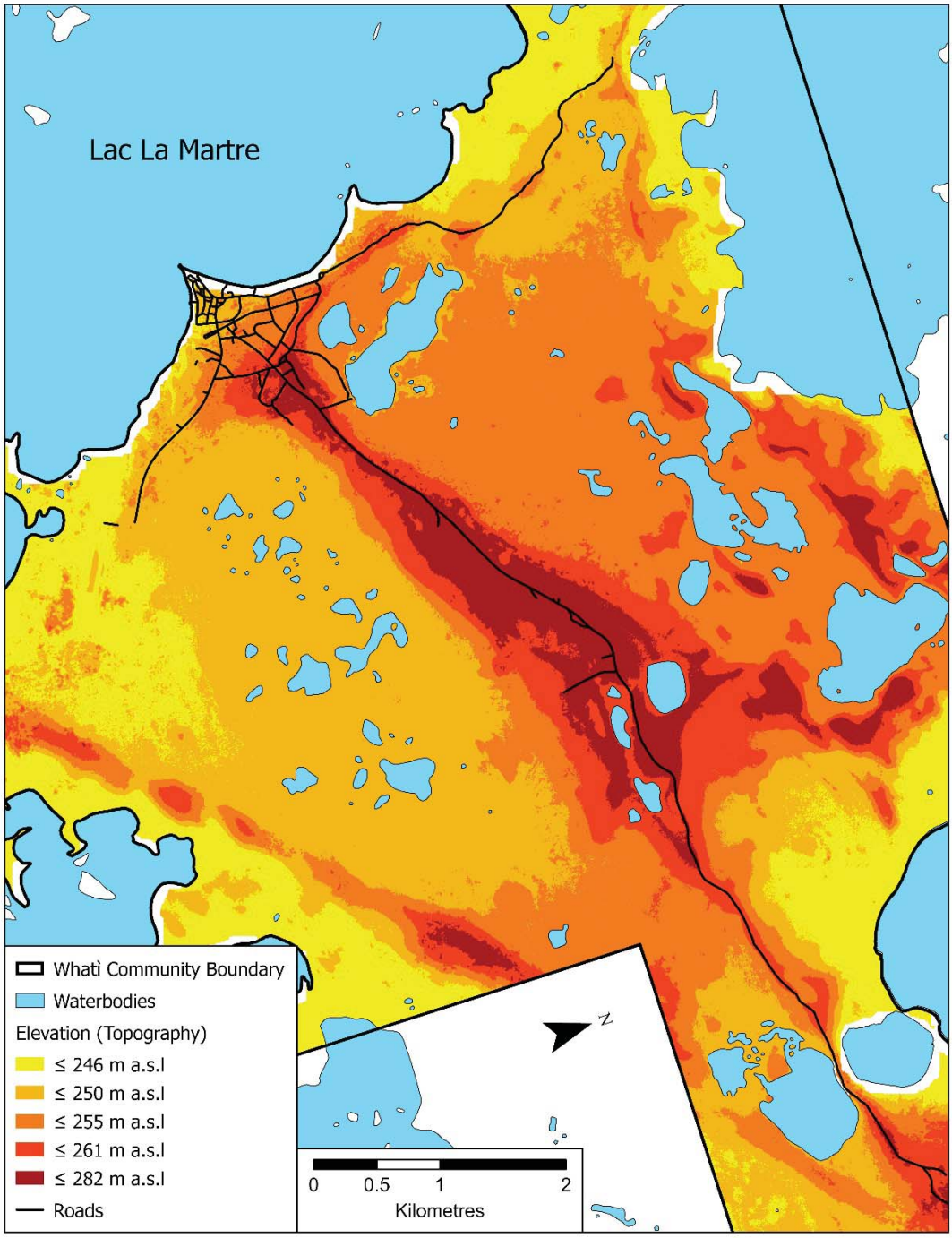

Figure 2.2 Elevation classes used as categorical inputs to represent topographic features in the model. The highest three classes (> 250) represent gravel features in the study area. This decision was informed by data collected and observations made in the field.

Whatì falls into the extensive discontinuous permafrost zone according to the permafrost map of Canada (Heginbottom et al., 1995), indicating that between 50-90 % of the ground is underlain by permafrost. Ground ice content is categorized as low (considered to be less than 10 % ice by volume of visible ice), in the upper 10-20 m (Heginbottom et al., 1995).

The main species of vegetation found throughout the study area are; spruce trees (Genus: *Picea*), deciduous trees such as aspen (*Populus*) and willow (*Salix*), Labrador tea (*Rhododendron*), buffaloberry (*Shepherdia*), fireweed (*Epilobium*), bearberry (*Arctostaphylos*) and mosses and lichens including peat moss (*Sphagnum*), reindeer lichen (*Cladonia*) and feathermoss (*Ptilium*) (Figure 2.3). The vegetation of the study area is mainly dependent on the local hydrology (drainage, water table, soil moisture) and can be considerably heterogeneous over short horizontal distances.

2014 was a record forest fire season. Roughly 84 % of the study area was affected by the fires with patches of unaffected vegetation. The fire stopped short of the built community due to anthropogenic and natural firebreaks.

2.4 Methods

2.4.1 Ground-Truth Pits

139 ground-truth pits (hereafter pits) were excavated during a 2019 field season (Figure 2.1). The data collected at these pits is used as the dependent variable in the model. Pit locations were sampled primarily off of vegetation rather than topographic features as vegetation cover is heterogeneous and is typically the main control on permafrost distribution in boreal environments (Fisher et al., 2016; Holloway et al., 2020).

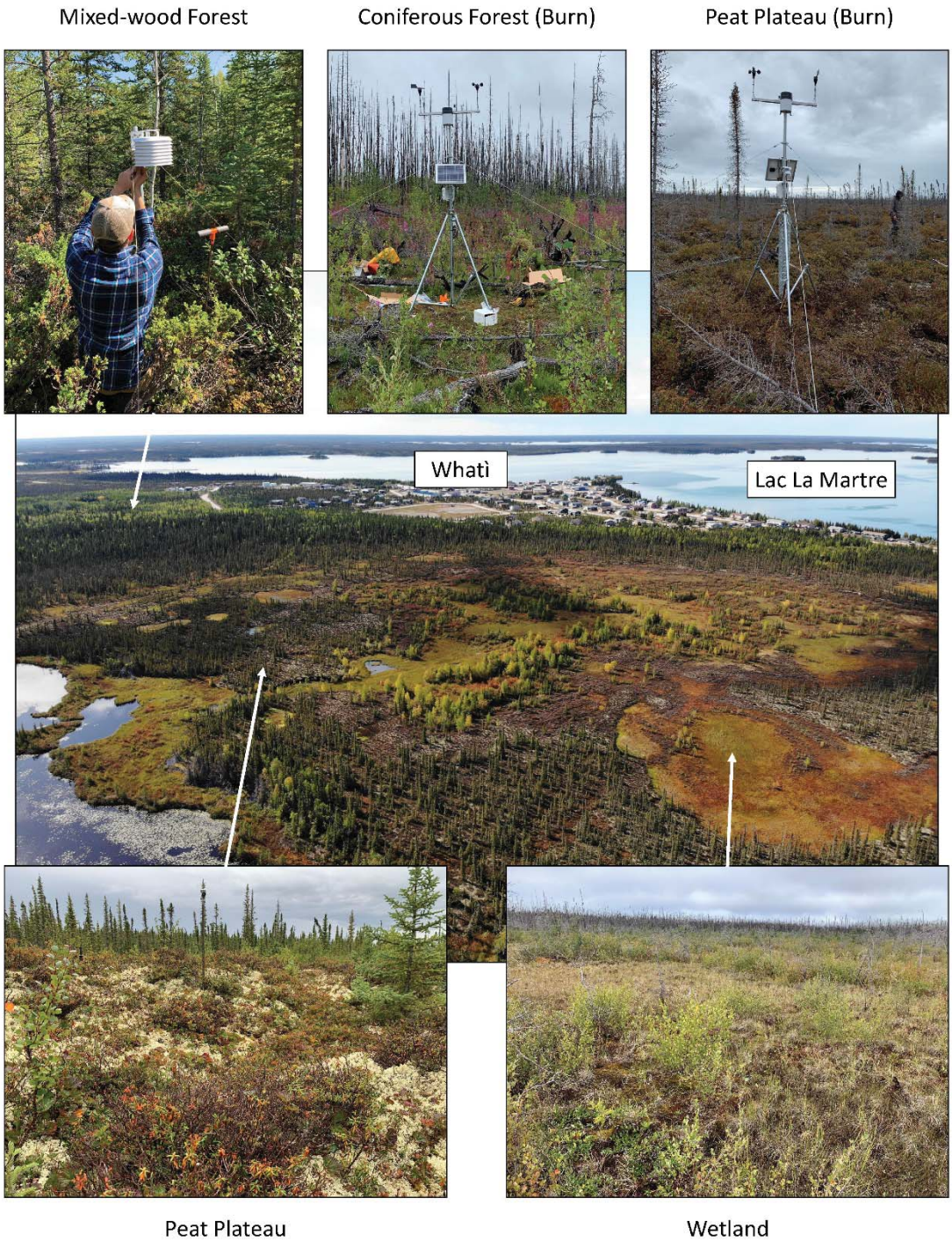

Figure 2.3 Common vegetation classes found throughout Whatì, NT. Examples of burned environment throughout the study area are not pictured in the larger image.

To efficiently create pits in the field, transects were created that passed through as many vegetation classes as possible with pits recorded approximately every 150 m or where vegetation or terrain sharply changed. The distribution of pits is limited by access as the environment is difficult to traverse. While the pits were recorded away from the influence of infrastructure (roads, off-road trails), the points are clustered around these areas due to accessibility.

2.4.1.1 Ground-Truth Pit Observations

Site observations at each pit included thermal profiles and major vegetation types, as we noted the ground cover type at each site, specifically the presence or absence of moss and lichen (*Sphagnum*, *Cladonia* and *Ptilium)* recorded as a binary variable (e.g. present or absent). Additional observations including site surroundings such as wetland, peat plateau, gravel features, or in an area affected by recent wildfires were recorded. We recorded GPS points using a handheld GPS (Garmin GPSMAP 64x Series) using waypoint averaging (accuracy of 1-4 m).

Pits were excavated in order to determine presence or absence of permafrost (Bonnaventure & Lewkowicz, 2008; Lewkowicz & Ednie, 2004). Upon arriving at the pit, a soil probe (1.6 cm x 10.2 cm Extendible Tile Probe Complete) or portable hammer-drill (DeWalt Flexvolt 60V MAX 4.0 cm Cordless SDS MAX, DCH481X2) was used to make a pilot hole with a target depth of 1.5 m (range of max depths of holes excavated: 30-189 cm). This was not always possible due to coarse substrate or the presence of permafrost before 1.5 m. This depth was chosen as previous studies indicate that active layer depths in the discontinuous permafrost region of the NT boreal forest rarely exceed 1.5 m however, they can extend to 2.0 m in less

common conditions (Nixon & Taylor, 1998; Wolfe, 1998). The deepest pit recorded during this field season was 189 cm.

Once the pilot hole was created, a temperature probe (Figure 2.4) consisting of a modified carbon fiber avalanche probe with four thermistor cables (E348-S-TMB-M006, accuracy: < ± 0.2 °C, resolution: < ± 0.03 °C) attached to it, was inserted into the hole to record a thermal profile. Internal thermistors cables were spaced at 0 cm, 25 cm and 50 cm from the maximum depth (Holloway & Lewkowicz, 2020) with an external thermistor used to measure the ground surface temperature. The internal cables, run through the probe and protrude out, pointing downwards at a forty-five-degree angle and are fixed in place with gorilla glue. In order to assure that the measurement is of ground temperature and not air temperature the soil probe is used to apply leverage against the thermal probe, driving the thermistor heads sideways into the ground at the max depth of the pilot hole.

Once the thermal probe was successfully inserted into the pilot hole all thermistor cables were plugged into a HOBO 4-Channel Analog Data Logger (UX120-006M, accuracy: ±0.15 °C, resolution: 0.002 °C). The amount of time to reach equilibrium (5-12 min) varied depending on the temperature, moisture content and substrate. Once all four channels were changing at a rate lower than one hundredth of a degree per one minute, values and depths were recorded (Bonnaventure et al., 2012; Holloway & Lewkowicz, 2020; Lewkowicz & Ednie, 2004).

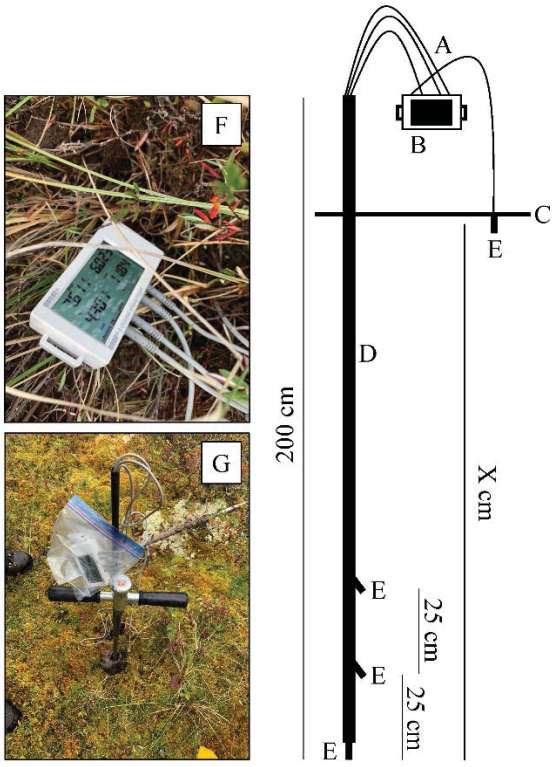

Figure 2.4 Schematic of Temperature probe used in the field. A) 4 thermistor cables used in the probe, 3 internal and one external. B) 4-channel logger used in the field (UX120-006M). C) Horizontal line representing the ground, D) The body of the temperature probe, mainly in the ground. E) Thermistor cable heads, this is where the measurement is recorded. F) Photo of 4-channel logger. G) Photo of temperature probe in use, the soil probe is in the ground to provide leverage to push the thermistor cable heads at an angle into the ground. X represents the depth of the probe which varies from pit to pit.

2.4.2 Analytical Methods

2.4.2.1 Field Data Processing

The probability modelling process involved a series of operations performed in statistical software SPSS (IBM Corp. Released 2013. IBM SPSS Statistics for Windows, Version 26.0. Armonk, NY: IBM Corp.) as well as ArcGIS Pro (ArcGIS Pro. Version 2.6.2, ESRI; 2020). Figure 2.5 is a flowchart depicting the order of operations performed to create the

final model. Three inputs a (vegetation observations, TPI and elevation) are identified as being independent variables whereas ground temperature is the dependent variable. Model input data was derived from data recorded at pits as well as optical imagery acquired from GeoEye on 17 September 2017 (Imagery © [2017] DigitalGlobe, Inc.).

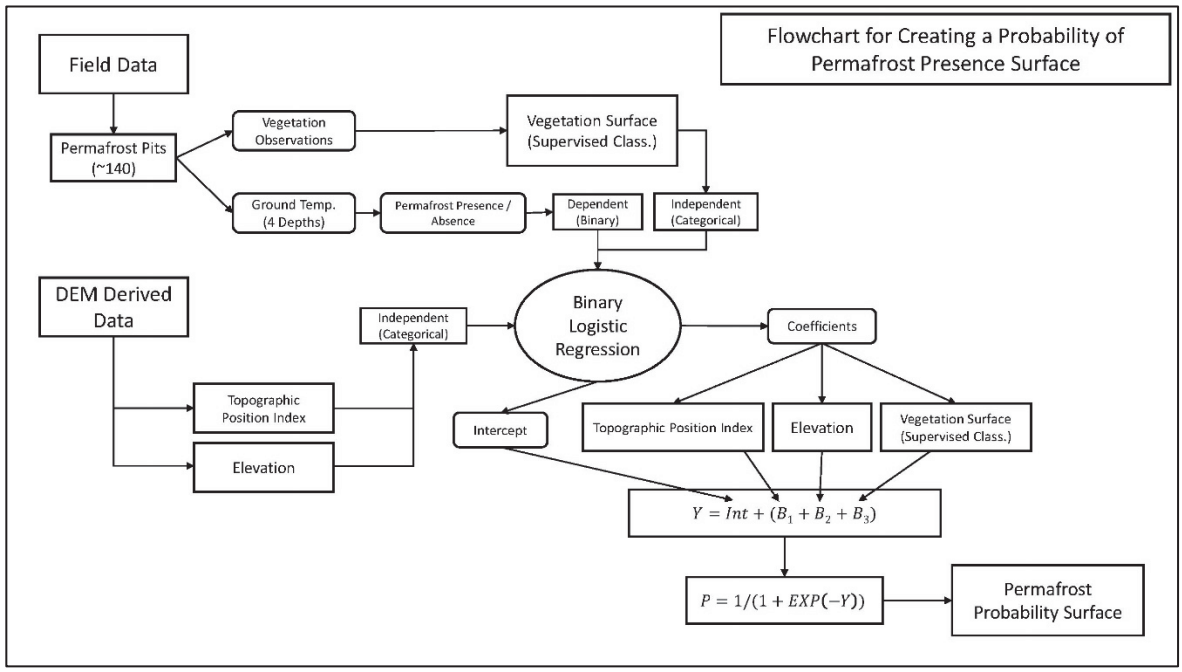

Figure 2.5 Depicts the order of operations used to generate a permafrost probability model.

The vegetation observations (plant species, ground cover) recorded at each pit were synthesized into different vegetation classes based on vegetation species occurrence. Vegetation classes where preliminary modelling showed that the burn influenced the presence or absence of permafrost were broken into burnt and not-burnt classes, thus coniferous forests, mixed-wood forests and peat plateaus were split into burnt and not-burnt classes. Peat plateaus showed little change in the modelled probability regardless of whether they were classed as burnt or not-burnt, however they remained separate as each of the two classes had high sample occurrence

(n = 26 and n = 16 respectively (Table 2.1). Low-shrub, organic matter and Low-shrub, clearing weren't split into burnt and not-burnt pairings as they showed little difference when modelled and had relatively low sample occurrence (n = 9 and n = 12, respectively).

Each pit that did not reach a depth of 1.5 m or indicate the presence of permafrost prior to 1.5 m (n = 31) was examined by plotting thermal gradient profiles in Excel. Here, the slope of the line was examined to determine if ground temperature would cross a threshold of 0.5 °C by a depth of 1.5 m (Bonnaventure & Lewkowicz, 2012; Lewkowicz & Ednie, 2004). Pits were categorized as permafrost present if 0 °C was crossed between a depth of 1.5 – 2 m (Holloway & Lewkowicz, 2020; Lewkowicz & Ednie, 2004).

2.4.2.2 Geospatial Data Processing

Independent variables used in the model are elevation, topographic position index (TPI; v. 1.3a, Jenness Enterprises, 2006) and vegetation class. The DEM derived variables (elevation, TPI) were obtained from a 2 m elevation model derived from GeoEye optical imagery taken on 17 September 2017 (Imagery © [2017] DigitalGlobe, Inc.). The elevation model was produced by the Polar Geospatial Center at the University of Minnesota using the surface extraction with TIN-based search and space minimization algorithm (Noh & Howat, 2017).

In this study the elevation variable was used as a proxy for mineral rich (gravel as well as larger stones) topographic features. The presence of well drained gravel/till is typically not associated with the presence of permafrost in discontinuous permafrost zones it was important to be able to capture this spatially (Romanovsky & Osterkamp, 1995; Shur & Jorgenson, 2007). A surficial geology map was not available at a comparable scale thus, elevation breaks (Table 2.1) were used as a proxy for the presence of gravel features which are the prominent

topographical features in the study area. This decision was made based on field observations which indicate that the main cause of relief in the study area is the presence of these features (possible eskers).

TPI shows the relative elevation of a cell compared to the surrounding cells, which is useful in locating topographic depressions. Standing water, which accumulates in low TPI areas, reduces the likelihood of permafrost if it remains year-round (Fisher et al., 2016; Higgins & Garon-Labrecque, 2018). Additionally, topographic depressions can capture drifting snow in winter, which prevents winter cooling of permafrost. Thus, areas with a deep snowpack are typically associated with warmer ground or permafrost temperatures (Bonnaventure et al., 2017; Way & Lewkowicz, 2018).

In order to include TPI and elevation in the binary logistic regression model individual raster surfaces were created for TPI and elevation. The TPI and Elevation surfaces were reclassified using natural breaks (jenks), which classes data into natural groupings (based on the data) in order to maximize differences between classes (De Smith et al., 2007). This was performed on the elevation surface to identify the presence of topographic features rather than using elevation in the traditional sense (temperature lapse rates). The extract by points tool in ArcGIS Pro was used to create a table that relates the TPI and elevation to the pits by location.

Available third-party vegetation classifications for the study had resolutions that were too coarse or vegetation classes that were too simple for use in this study area. Thus, vegetation field observations were used to inform a supervised classification on satellite imagery to derive a spatially complete vegetation map in ENVI (ENVI. Version 5.5, L3 Harris Geospatial Solutions; 2008)

Table 2.1 Model input variables, including classes, descriptions and coefficients obtained through permafrost probability modelling. The number of pits within each class is shown as n. The constant reported in the bottom right of the table is the intercept provided by the binary logistic regression model. It is a constant in the probability equation used to convert from the coefficients reported in this model to probability.

Variables	Class	Description	Coefficient
Vegetation Classification	**Coniferous Forest** (CC) (n = 19)	Black spruce and tamarack tree stands w/, organic mat. layer including moss, lichen, Labrador tea, cinquefoil	90.8
	Coniferous Forest (Burn) (CCB) (n = 14)	Same as *Coniferous Forest* with grass of Parnassus, sedges and horsetails. Visible evidence of recent burn (2014).	50.3
	Low-shrub, Clearing (LSC) (n = 12)	Low density paper birch, willow. rose, horsetail, fireweed and grass.	50.3
	Low-Shrub, Organic Mat. (LSOM) n = 9)	Coniferous Forest adjacent, similar organic mat., low density to no tree cover. Juniper, willow, spruce, Labrador tea, moss, lichen, cinquefoil.	54.2
	Mixed-Wooded Forest (MW) (n = 17)	Aspen, birch, willow, spruce, alder w/ thin organic mat. layer. Rose, buffalo berry, bear berry, occasion thin layer of moss and lichen.	52.8
	Mixed-Wooded Forest (Burn) (MWB) (n = 12)	Same as *Mixed-Wood Forest* w/ fireweed. Visible evidence of recent burn (2014).	50.2
	Peat Plateau (PP) (n = 16)	Visible plateau or hummocky terrain. Cloudberry, Bog Rosemary, White Lichen, Moss, Labrador tea, Spruce tree stands.	73.9
	Peat Plateau (Burn) (PPB) (n = 26)	Same as *Peat Plateau* with visible evidence of burn (2014).	86.1
	Wetland (WL) (n =14)	Wet Moss layer, Grass, Bog Birch, Fireweed, Sundew, Wax mertle, Willow, Cinquefoil, Bog Rosemary. High water table. Minimal resistance to soil probe.	50.9
Elevation*	1 (n = 13)	≤ 246.8 m asl.	50.0
	2 (n = 54)	≤ 250.5 m asl.	13.7
	3 (n = 52)	≤ 255.3 m asl.	16.4
	4 (n = 16)	≤ 261.9 m asl.	13.5
	5 (n = 4)	≤ 282.7 m asl.	0.0
Topographic Positioning Index (TPI)	1 (n = 11)	≤ -0.8	-5.2
	2 (n = 76	≤ 0.0	13.1
	3 (n = 48)	≤ 1.1	15.0
	4 (n = 4)	≤ 8.9	0.0
Constant			-81.2

* Elevation in this instance is being used as a proxy for surficial geology as major topography in the study area is dependant of surficial geology and our data suggested that surficial geology has an effect or the presence of permafrost.

The supervised classification used the maximum likelihood algorithm and was performed on an image stack made up of R, G, B, and NIR bands from the above mentioned GeoEye image, along with a derived layer from the normalized difference vegetation index (Tucker & Sellers, 1986). The vegetation classification was smoothed with a kernel size of 3 by 3 pixels and aggregate minimum size of 9 pixels to clean up the classification.

2.4.2.3 Binary Logistic Regression Model

In SPSS Statistics, a random sampling regime was used on the table which included vegetation, TPI, elevation and permafrost presence (0 or 1) for each of the 139 pits. The regime generated ten randomly sampled cross-validation pairs of testing and training data from the 139 pits. The pairs were split 33 and 67 % respectively. The full dataset was run in SPSS through the Binary Logistic Regression Model (BLRM) tool.

This model will establish a relationship between permafrost presence (dependent) and independent variables (Veg., Elev., TPI) (Deluigi et al., 2017). BLRMs work with both continuous and categorical variables (David W & Stanley, 2000). The BLRM generated coefficients for each variable as well as an intercept to determine the relative importance of each factor. The coefficients are represented by B_i and the intercept is represented by *int* in equation 1 (Panda et al., 2010). This equation (2.1) converts the coefficients and intercept into a probability value which represents the probability of achieving 1 (permafrost present).

$$P = \frac{1}{1 - e^{-(int + \sum_1^n B_i)}} \qquad (2.1)$$

2.4.2.4 Model Cross Validation

Different iterations of the model (10 random samplings of training data) were run in SPSS. Of the ten cross-validation pairs only one would be used to generate the final permafrost probability surface. In order to determine which pair yielded the best results four measures were observed:

Nagelkerke r-square (range of results: 0.81-0.88) which is a pseudo r-squared measurement used in regression models with a categorical dependent variable. Nagelkerke r-square ranges from 0-1, with the value representing how much of the variance in the dependent variable is explained by the independent variables. A higher r-square value means that more variance is explained by the model (Nagelkerke, 1991).

Hosmer and Lemshow significance test (range of results: 0.52-1.00). This significance test is a goodness-of-fit test used for binary dependent variables. It works by comparing p-values (sig.) to a chi-square value. If the significance value is greater than a threshold (> 0.05) the model is assumed to fit the data well, or rather, the opposite is rejected (Hosmer et al., 2013).

The accuracy of the BLRM (referred to as percentage correct) (range of results: 88.2 - 94.6 %), and the accuracy of the testing data (referred to as agreement) (range of results: 80.4 - 89.1 %) (Table 2.2). "Percentage correct" was provided by the BLRM tool in SPSS and measures the accuracy of the BLRM when applied to the training data (Table 2.3). Agreement was calculated in excel and represents the accuracy of the testing subsample when the model coefficients generated by the BLRM are applied to them (Table 2.3). Table 2.3 shows a breakdown of the model accuracy of the training and testing data for testing pair #7.

Table 2.2 Results of each binary logistic regression model run in SPSS using each cross-validation pair. The highest values for each category are highlighted in light grey and in bold. VO refers to a model run using the random sampling pair for run 7 but only using vegetation as a model input.

Run #	Nagelkerke R-square	H&L Sig. Test	Percentage Correct	Agreement	Average Value	Average Accuracy
1	0.81	0.89	88.2	**89.1**	87.0	88.7
2	0.88	0.95	92.9	80.4	89.1	86.7
3	0.83	0.99	90.3	82.6	88.8	86.5
4	0.85	0.99	92.5	84.8	90.4	88.7
5	0.85	0.99	90.3	80.4	88.8	85.4
6	**0.88**	0.99	93.5	80.4	90.4	87.0
7	0.86	**1.00**	91.4	87.0	**91.0**	**89.2**
8	0.86	0.52	92.5	82.6	78.3	87.6
9	0.82	0.52	91.4	84.8	77.6	88.1
10	0.88	0.99	**94.6**	80.4	90.7	87.5
VO	0.78	1.00	89.2	84.8	87.9	87.0

Table 2.3 Accuracy of the training and testing data for run seven shown in Table 2.1.

Observed		Predicted					
		Training data (% correct)			Testing data (Agreement)		
		Permafrost		Correct (%)	Permafrost		Correct (%)
		Absent	Present		Absent	Present	
Permafrost	**Absent**	36	4**	90	15	1**	93.8
	Present	4*	49	92.5	5*	25	83.3
	Overall (%)			91.4			88.5

* false positive

** false negative

The 4 measures were relatively consistent across all 10 of the pairs. The only measure with a significant range was the Hosmer and Lemshow significance test (range: 0.52-1.00), which was 0.52 for cross-validation pairs 8 and 9. The testing pair selected for use in the study

was number 7 in table 2.2. This run has the highest average value of 91.0 % (the average of all 4 measures with r-square and significance test adjusted to be out of 100) and the highest average accuracy (89.2 %, average of percentage correct and agreement; Table 2.2).

2.4.2.5 Permafrost Probability Model

The permafrost probability model was created by reclassifying the raster surfaces of the independent variables (Vegetation, elevation, TPI) to represent the coefficients obtained from the BLRM in SPSS. These were then inserted into equation 2.1 in the ArcGIS Pro raster calculator to create the final permafrost probability surface. This yielded a 2 m resolution raster that displays the percent probability of permafrost being present in any given pixel.

2.5 Results

2.5.1 Field Results

Of the 139 pits created during the 2019 field season, 83 were recorded as being permafrost present (either initially in the field or in post processing) whereas 56 were permafrost absent. Vegetation observations were recorded and synthesized into 9 unique classes. The classes are burnt coniferous forest, coniferous forest, low-shrub clearing, low-shrub organic matter mixed-wood forest, burnt mixed-wood forest, peat plateau, burnt peat plateau and wetland. One-time measurements of active layer depth (ALD) were recorded in the field at each pit (August 2019). Analysis of this data showed that ALD in the study area ranges from 40 cm to 180 cm. Figure 2.6 shows ALD statistics for each vegetation class.

2.5.2 Vegetation Classification

Landcover percentages in the study area are shown in figure 2.7B. Vegetation covers 84.9 % of the study area with the remaining 15.1 % representing waterbodies (13.3 %) and

infrastructure (1.8 %). Wetlands make up 34.9 % of the vegetation cover, burnt mixed-wood forest makes up 19.5 % and low-shrub, organic matter makes up 12.7 %. Burnt coniferous, burnt peat plateau and coniferous forests each cover 8.9 %, 9.6 % and 8.7 % respectively (Figure 2.7).

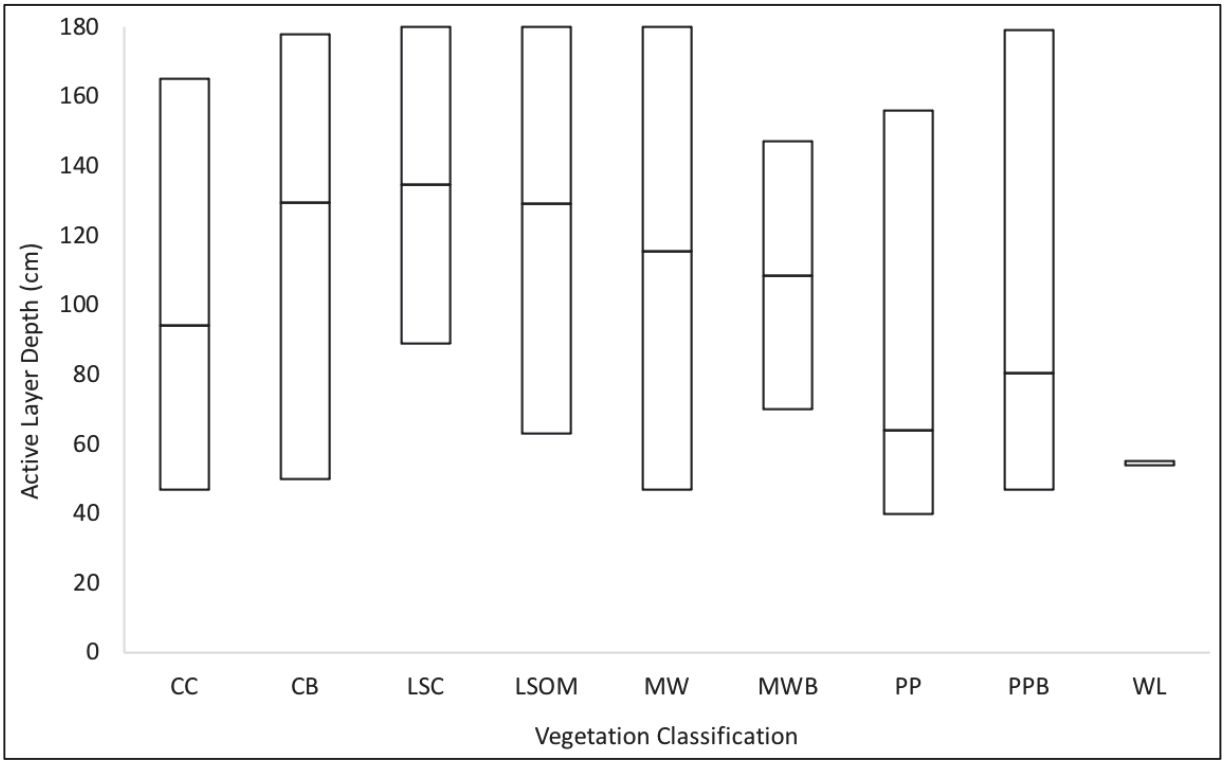

Figure 2.6 Shows the average active layer depth (cm) recorded at the pits for each vegetation class. Range of depths are also shown.

2.5.3 Model Output

The probability map (Figure 2.8) shows the likely spatial distribution of permafrost within the community boundary of Whatì. It predicts that 50.0 % of the study area is underlain by permafrost with 10 % of the pixels having a probability of less than 1 % (~0 % chance) and 36 % having a probability of greater than 99 % (~ 100 % chance). The distribution of permafrost in the study area is skewed towards the upper and lower extremes, 32 % of pixels fall between

1 – 25 % and 10 % fall between 75-99 %. The middle values representing probability between 25-75 % contains only 12 % of the pixels in the permafrost probability map (Figure 2.8B).

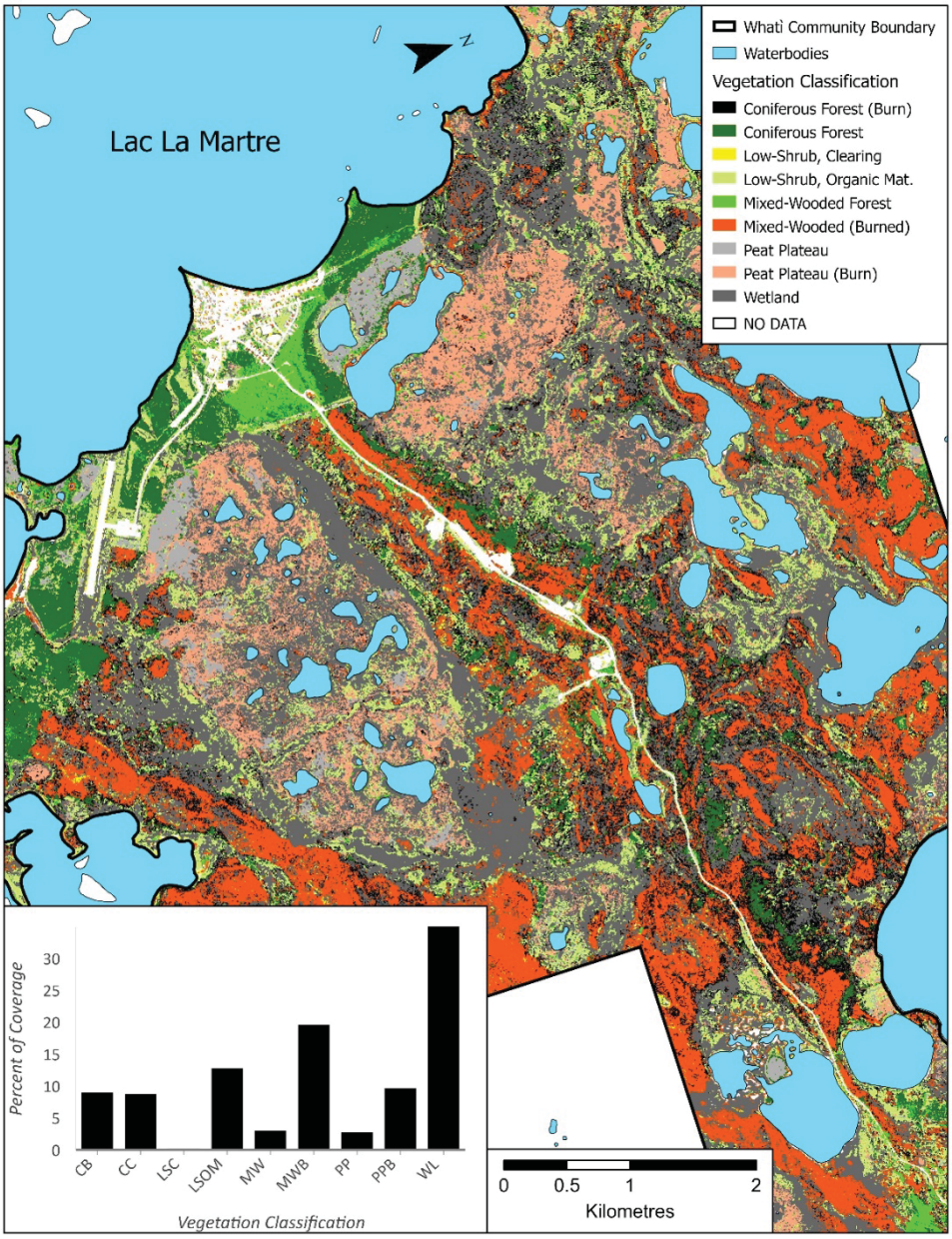

Figure 2.7 A: Vegetation classification created in ENVI. B: Graph showing the percent occurrence of each class in the vegetation classification surface. Coniferous Forest (Burnt) = CB, Coniferous Forest = CC, LowShrub, Clearing = LSC, Low-Shrub, Organic Matter = LSOM a class that represents a similar forest floor to coniferous forests, without the tree cover, Mixed-Wood Forest = MW, Mixed-Wood Forest (Burnt) = MWB, Peat Plateau = PP, Peat Plateau (Burnt) = PPB, Wetland = WL.

Of the three variables used in the model, vegetation has the greatest influence on the probability surface. This is evident as the magnitude of coefficients is far greater for vegetation (50.2 – 90.8; Table 2.1) than for either elevation or TPI (-5.2 – 50.0; Table 2.1).

Higher coefficients lead to higher permafrost probabilities as the intercept in this model is -81.2. The vegetation classes most likely to predict permafrost presence were low-shrub organic matter (71.0 % of area classified as permafrost), peat plateau (99.0 %), burnt peat plateau (99.9 %) and coniferous forest (100.0 %). These four classes account for 32.9 % of the probability map. The wetlands vegetation classification (32.3 % of area classified as permafrost present) accounts for 36.6 % of the surface (Figure 2.9).

Despite the wetland class having a low permafrost probability, it covers such a large area that it contains 11.8 % of the permafrost in the study area. The remaining classes; low-shrub clearing (30.9 % permafrost probability), mixed-wood burnt (26.1 %), mixed-wood (36.8 %) and coniferous forests burnt (34.0 %) make up 30.5 % of the probability map.

2.5.4 Model Simplification

The permafrost probability model was simplified using coefficients from a BLRM created with only vegetation acting as an independent variable. The simplified model is termed the Vegetation Only (VO) model and compared to the All Variables (AV) model (AV = permafrost probability model). This model is being evaluated to assess the usability of a vegetation only model for possible transfer to the adjacent environments as a first-order permafrost assessment. The statistical measures for the VO model are found in Table 2.2.

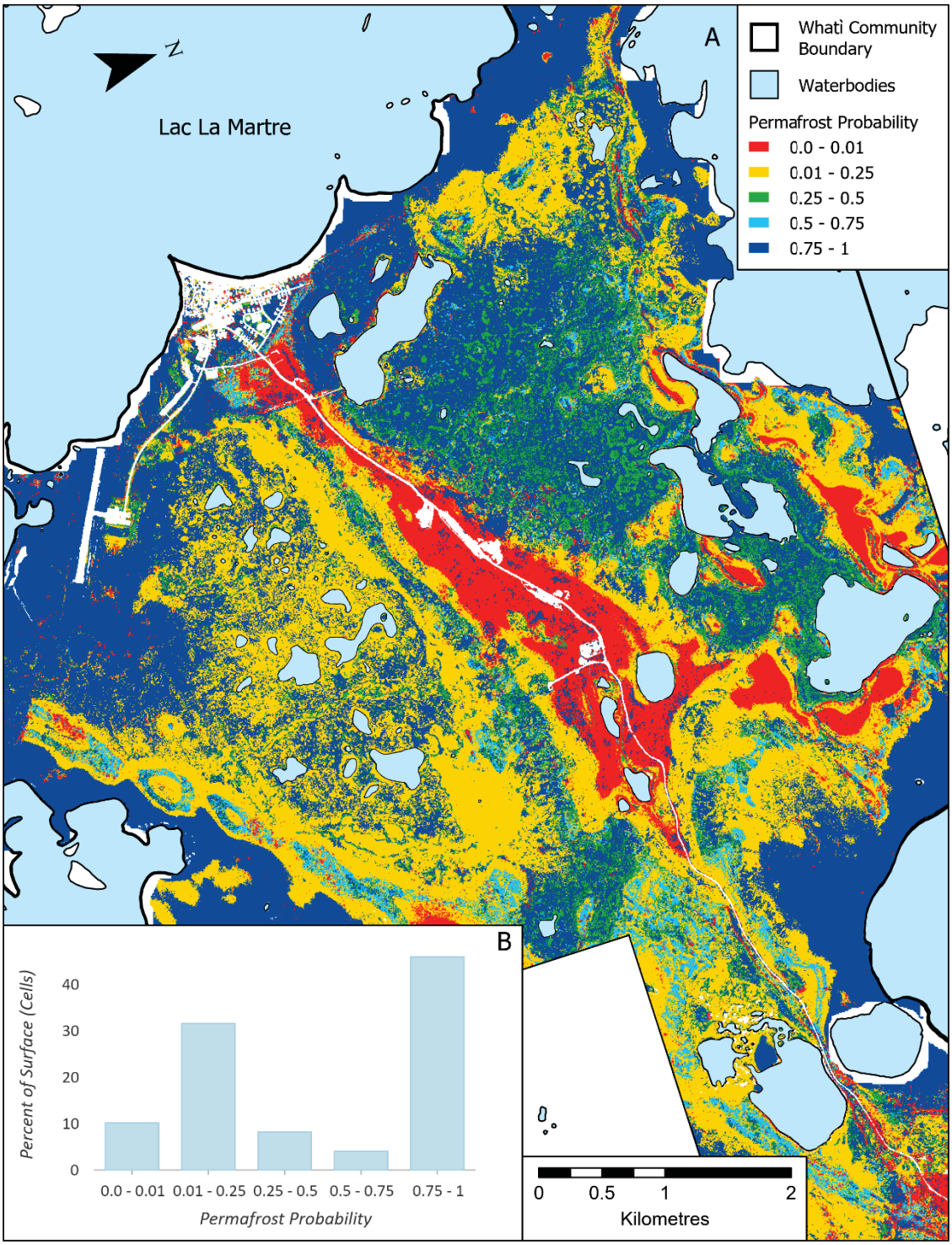

Figure 2.8 A) Permafrost probability surface generated for the community of Whatì. B) Histogram showing percent coverage of permafrost probabilities across the study area.

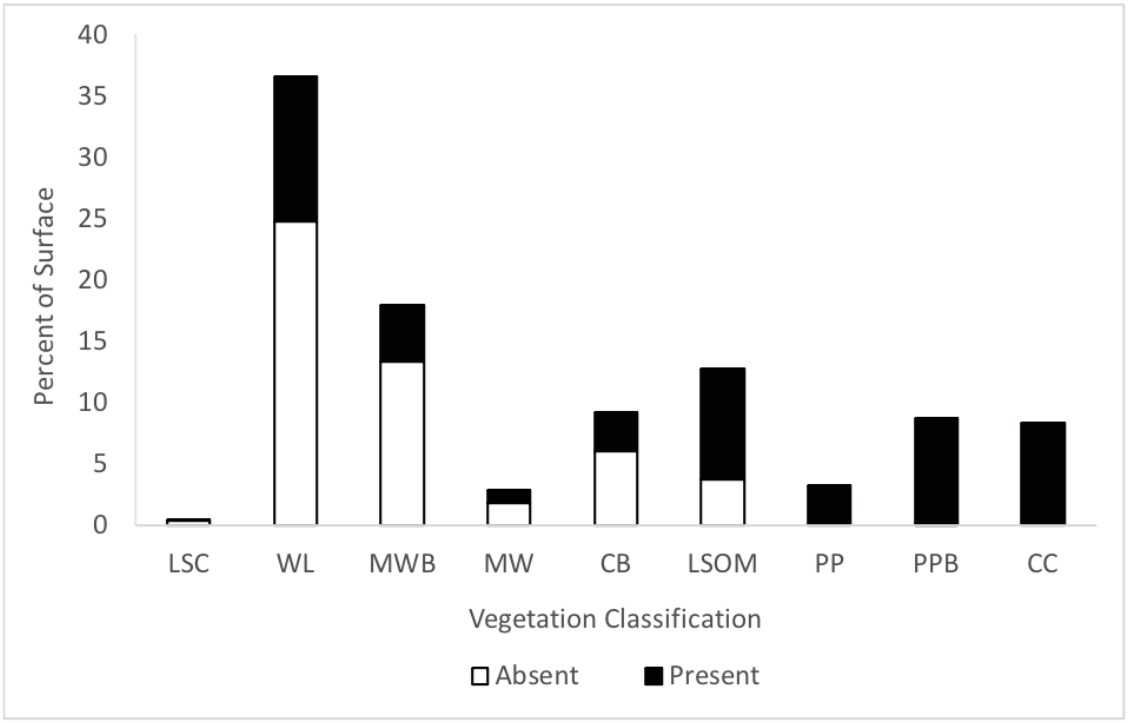

Figure 2.9 Shows the breakdown of cells classified as permafrost present and absent and their percent contribution to the final probability surface for each vegetation class.

Despite lacking two of the three variables included in the AV model, the VO model does not report the worst values in any of the statistical measures except for the r-square value. The VO model reported an r-square value of 0.78 whereas the AV model reported 0.86 (Table 2.2).

The results of the VO model were compared to the measure of permafrost presence of absence in the pit data. The VO model has an agreement of 62.8 % compared to an agreement of 72.8 % for the AV model. This change of 10 % represents a degree of error that could be avoided by including elevation and TPI. VO and AV were differenced in order to visualize the spatial location of the main areas of dissimilarity (Figure 2.10). In figure 2.10 it is evident that the majority of permafrost probability differences are minor (mean between +20 % and -20 %).

Only the extremes of the difference surface represent a change from permafrost presence to absence or vice versa.

2.6 Discussion

2.6.1 Model Accuracy Assessment

While the binary logistic regression model has an accuracy of 91.4 % (Table 2.3), this does not represent the accuracy of the probability model. To assess this, the generated probability surface (Figure 2.8) was compared to the assessment of permafrost presence in the pits (n = 139). Agreement (%) was based on whether the probability model agreed with the assessment of presence / absence in the GTPs. The agreement value is 72.8 %. The disagreement (27.2 %) could be caused by errors in data collection however they are most likely due to errors in the vegetation classification or possibly a control on permafrost presence that isn't captured in the model.

2.6.2 Comparison to Existing Permafrost Information

Permafrost is often mapped at broad scales due to the difficulty of ground truth data collection leading to poorly resolved permafrost distribution maps with high uncertainties. Before this study, the only maps of permafrost distribution around Whatí available were at best 1 km^2 resolution (Obu et al., 2019). The sources of comparison used for permafrost distribution are the Permafrost Map of Canada (Heginbottom et al., 1995), as well as the recent publication of circumpolar permafrost distribution by Obu et al. (2019). This is because they are commonly known and relied on in the field of permafrost science in Canada and there aren't other products at a scale more comparable to the Whatì model. These models are more appropriate for regional

permafrost mapping and the Whatì model shows the permafrost probability distribution at a spatial scale more useful for local development decisions.

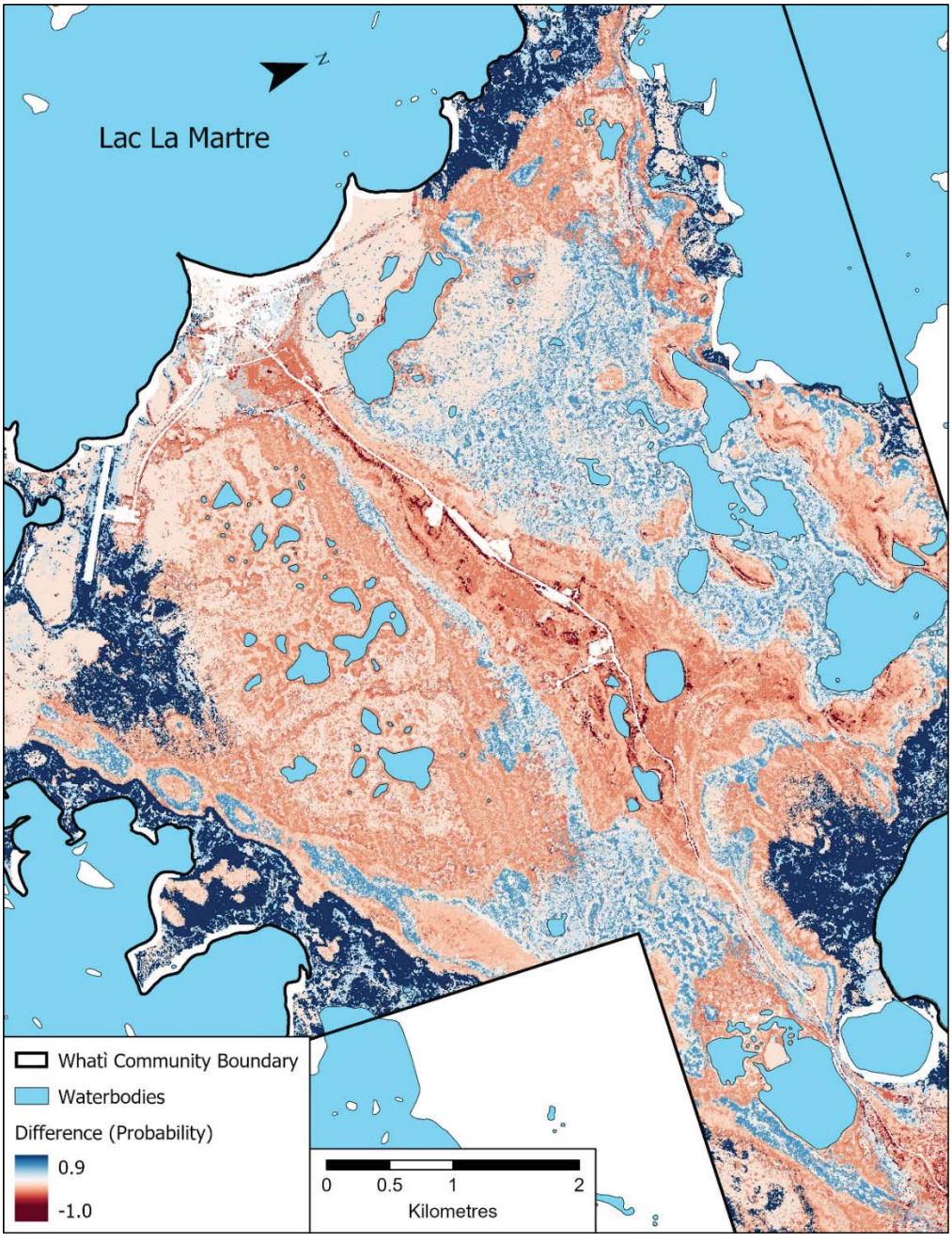

Figure 2.10 Probability difference surface created by subtracting the Only Vegetation surface from the All-Variable surface (AV-OV).

The Heginbottom et al. (1995) map was hand drawn at a national scale (1:7,500,000) using a combination of geotechnical information and climate indices. While this map is useful to describe regional patterns, it is now more than 25 years old and uses a continuity permafrost classification based on spatial coverage (e.g. continuous, extensive discontinuous, etc.), making it challenging to apply at scales useful to inform development decisions.

In this map Whatì falls into the extensive discontinuous class, signifying that 50-90 % of the landscape is underlain by permafrost. Our model predicts that 50.0 % of our study area is underlain by permafrost, at the lower end of the Heginbottom estimate. Given the 2 m spatial resolution of the probability model presented in this paper, more information is provided about the location of the permafrost in Whatí.

The Obu et al. (2019) model used three input datasets: Mean Annual Ground Temperature (MAGT), permafrost zones, and permafrost probability acquired from remotely sensed sources. According to these data, Whatì has a MAGT between -1 °C and -2 °C, falls into the discontinuous permafrost zone (50 – 90 % coverage), and has a permafrost probability of 75 – 90 %. Our high-resolution model broadly agrees with these results but provides more detail based on local variations in topography and vegetation.

2.6.3 Ecosystem-Permafrost Interactions

Natural and anthropogenic disturbances are typical in boreal environments and can impact permafrost distribution and the development of thermokarst (Fedorov et al., 1998; Jin et al., 2008; Osterkamp et al., 2009). A study by Shur and Jorgenson (2007) outlined a conceptual system of classifying permafrost landscapes based on the interactions between climate, ecosystem structure and rate of succession following disturbance. In this classification scheme,

Whatì is classified as climate-driven, ecosystem-modified. Whatì falls within this classification with a MAAT of -5 °C (Wang et al., 2016), supporting the existence of permafrost. However, permafrost distribution is modified by the structure of the surrounding ecology. Similar environments with warmer MAATs (>0 °C) are classed as "ecosystem protected" with permafrost existing due to the preservation potential of the vegetation in the ecosystem (Shur & Jorgenson, 2007).

Whatì's classification can be illustrated by looking at the field data. Land cover classifications defined by moss, peat and saturated organic soil are coniferous forest, low-shrub organic matter, peat plateau and burnt peat plateau which have 100, 78, 100 and 100 percent permafrost occurrence in the pit data respectively. Low-shrub clearing, mixed-wood and burnt mixed-wood classes are defined by mineral rich soil and minimal ground vegetation cover have permafrost occurrences of 17, 24 and 17 percent respectively. The low occurrence of permafrost in these classes is reflected in the results of the model (Figure 2.11).

2.6.4 Burn Analysis and Ecosystem Robustness to Permafrost Change

In the last century, forest fires in the northern boreal forest have increased both in severity and frequency (Kasischke et al., 2010; X. Wang et al., 2015). In 1950 boreal fires in North America burned at a rate of 1 million ha/yr, by the year 2000 that rate had tripled to 3 million ha/yr (Kasischke & Stocks, 2012). From 2009 to 2019 the average yearly forest fire burn by area (ha) in Canada was 2.7 million ha, much of the burn taking place in the boreal forest (Government of Canada. 2020, December 16. Indicator: Forest Fires. https://www.nrcan.gc.ca/our-natural-resources/forests-forestry). As such, understanding how

permafrost responds to fire disturbance is key to understanding the evolution of its spatial distribution.

The modelled coefficients of three vegetation classes contained variations depending on whether it experienced recent burn or not (Table 2.1). Of these classes coniferous forests (coefficients: not-burnt, 90.79; burnt, 50.29) represented the most substantial change in predicted permafrost probability when shifting from not-burnt to burnt. Mixed-wood (coefficients: not-burnt, 52.75; burnt, 50.17) and Peat Plateau (coefficients: not burnt, 73.92; burnt, 86.05) only changed marginally.

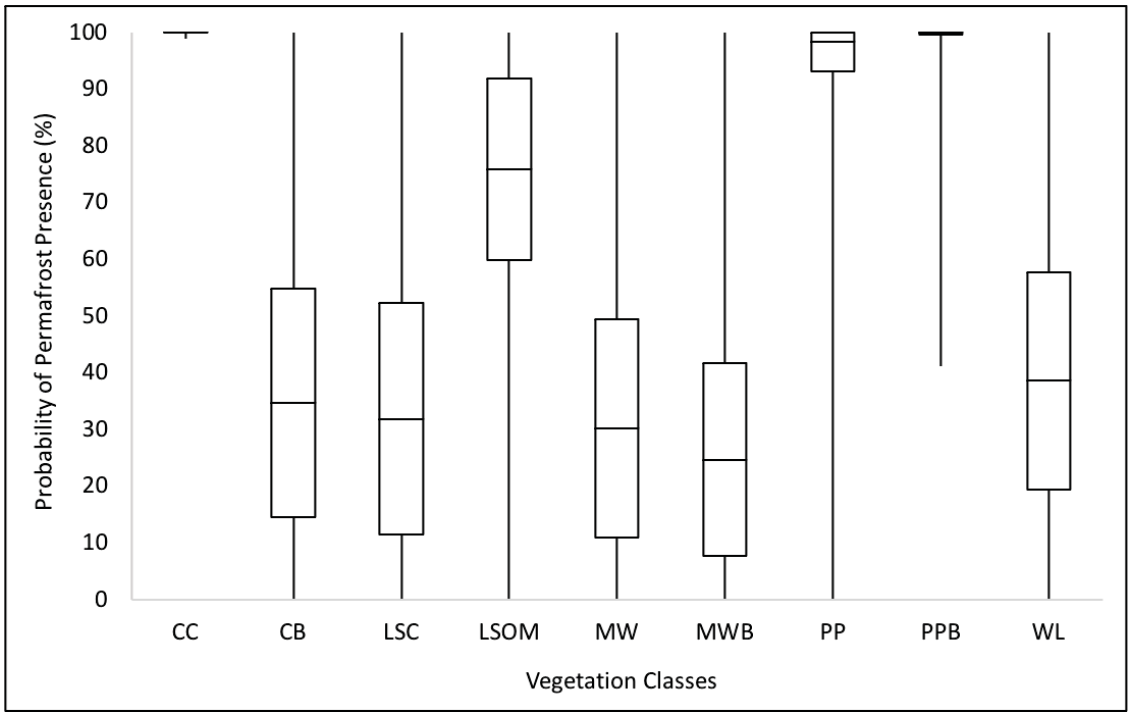

Figure 2.11 Shows the distribution (range, average, standard deviation) of permafrost probability generated by the model for each vegetation class.

To examine the potential impact of fire on permafrost distribution in the study area, two model scenarios were tested; 1) the entire landscape burns ($burn_{100}$) and 2) none of the landscape

burned (i.e. vegetation state before the 2014 fire; $burn_0$). Compared to the probability model, which shows an average permafrost probability of 50.0 %, $burn_{100}$ results in a reduction in permafrost coverage of 6.2 % to 43.8 %. $Burn_0$ resulted in an increase in coverage of 12.1 % to 62.1 %. These scenarios illustrate the impact fire can have in determining the future permafrost distribution in Whatí. Whether or not Whatí experiences fire in the coming decades will be one of the key determining factors of the future of Whatí's permafrost.

The effects of fire on permafrost vary greatly and are typically dependent on both antecedent conditions and burn severity (Shur & Jorgenson, 2007). The most important factors influencing post fire permafrost stability are antecedent organic layer thickness, remaining organic layer thickness post-fire, post fire soil moisture content and the speed of vegetation succession and regrowth to pre-fire conditions (Fisher et al., 2016; Jiang et al., 2015; Yi et al., 2010). Results from the probability model support this as peat plateau shows very little difference in the probability of permafrost regardless of its burnt status (Figure 2.11).

Peatlands are often more resilient to fire as they typically have a higher soil moisture content due to poorly drained fine-grained soils (Genet et al., 2013; Jafarov et al., 2013; Zhang et al., 2015), there is also the possibility for near-surface permafrost preventing drainage causing a high water table which also increases resiliency to deep burns (Turetsky et al., 2011). This is apparent in a comparison of ALD between burnt peat-plateau (80.5 cm) and peat plateau (64.0 cm), which represents a difference of 16.5 cm (Figure 2.6). In areas of low burn severity, where moss and other surface organics remain, the effect of the burn may be less severe and moss could fully recover in 2-3 decades (Turetsky et al., 2010).

Despite their resilience, burns in peatlands can have long-lasting effects if fire causes thermokarst to develop (Genet et al., 2013; Jafarov et al., 2013; Zhang et al., 2015). Progressive thaw in peatlands can increase talik extent from 20 % to 70 – 100 % in burnt sections (Gibson et al., 2018). Thermokarst recovery can take centuries and permafrost will not return until the talik has drained, and the conditions support permafrost aggradation (Gibson et al., 2018). This is especially concerning as much of the study area is classified as complex peat plateau or wetland environments.

In burnt forests, the reduction in the tree canopy resulting in decreased snow interception is considered to be one of the greatest factors leading to the degradation of permafrost and thickening of the active layer (Smith et al., 2015). This provides an explanation for why the greatest change (coefficients: not-burnt, 90.79; burnt, 50.29) due to burn is observed in coniferous forests where tree stands were burned, reducing interception to near zero, and organic ground cover was not as thick as in the peat plateaus.

As the probability model does not involve climate inputs it cannot be projected for future climate scenarios, however they are still worth discussing in the context of this model. In particular we want to explore whether the rate of ecosystem succession is fast enough to combat the speed of predicted warming.

RCP4.5 and RCP8.5 (Wang et al., 2015; Wang et al., 2016) projections were examined for the study area for the 2050 (2041-2060) and 2080 (2071-2100) forecasted climate normals. With a starting MAAT of -5 °C (1981-2010) RCP4.5 predicted a MAAT of -2.2 (Δ +2.8) for 2050 and -1.4 °C (Δ +3.6) for 2080 (Wang et al., 2015; Wang et al., 2016). While RCP8.5

predicts a MAAT of -1.1 °C (Δ +3.9) and 1.6 °C (Δ +6.6) for 2050 and 2080 respectively (Wang et al., 2015; Wang et al., 2016).

Smith et al. (2015) concluded that regrowth of a boreal environment after a burn would take 50 years and a predicted rise in MAAT of 3 °C (MAAT of 1981-2010 climate normal for Smith et al.'s study area = -5.1 °C) over that span was enough that permafrost in burnt environments would most likely not return to pre-burn conditions until complete regrowth occurs. Looking at the 2050 projection for RCP4.5 the rise in temperature is +2.8 °C for Whatí, this is just short of that 3 °C threshold. However, RCP8.5 represents a rise of 3.6 °C, well past the threshold. This indicates that in the 50 years from the 2014 burn in Whatì, MAAT is expected to increase by at least 2.8 °C, which could prevent permafrost from returning to pre-burn conditions until the ecosystem also returns to pre-burn conditions (Smith et al., 2015).

2.6.5 Uncertainty and Improvements

As this study is intended to create a method for improving community-scale permafrost knowledge at minimum cost and effort it is important to assess uncertainties, areas of improvements and pitfalls. Due to the lack of previous research in our study area, there were some clear and avoidable missteps that could have had downstream effects on the model. The number of pits across all vegetation types was uneven due to limitations to traversal and access in the field.

This issue was also faced with the elevation variable, specifically elevation class 1, which according to the model has a great modifying effect on the probability of permafrost (Table 2.1). While this effect can be justified through the literature, it is certainly worth noting

that this class was only sampled 13 times across the 139 pits used in the final analysis. This could lead to the conclusion that outlier pits are influencing the coefficient for this class.

The vegetation classification has the potential to be a source of uncertainty across the study area. As the vegetation class variable has such a high influence on the probability value, a pixel misclassified in the vegetation classification surface can lead to inaccuracies in the permafrost probability surface. Incorporating one or a combination of coarser resolution remote sensing products such as airborne thermal or multispectral data could improve the classification (Fuentes et al., 2001; Larsen et al., 2009; Price, 1981). RADAR or LiDAR could have aided as the structure of wetlands would vary significantly from other classes such as CB (Chasmer et al., 2014; Korpela et al., 2009; Morsdorf et al., 2004) This may have resulted in a different classification with more confidence, however these methods are considerably more expensive and therefore defeat one of the key purposes of the study.

To understand the uncertainty introduced by the vegetation classification surface, the distribution of probabilities throughout vegetation classes (Figure 2.11) can be explored. The three classes that recorded permafrost presence in all the pits (field): peat plateau, burnt peat plateau and coniferous forest display the highest permafrost probabilities in the BLRM. Coniferous forests have the mean of 99.0 % and a range of 1 %. Burnt peat plateaus have a mean of 99 %, and a range of 59 %. Peat plateaus have a range of 99 % and a mean of 98 %. In this situation we see that the extremes don't affect the means substantially, however they do provide a question to examine: if these three classes recorded only occurrences of permafrost at the pits why are they different?

In the VO model these classes have the exact same coefficients (42.4, with a constant of -21.2). However, in the AV model their coefficients are slightly different (Table 2.2), suggesting the differences are due to interactions with elevation and TPI. The only way that coniferous forest (coefficient = 90.8) would predict a slightly lower probability value is with a combination of elevation class 5 (coefficient = 0.0), and TPI classes 1 (coefficient = -5.2). This is a possible combination as nothing we saw in the field suggests that this combination of vegetation, TPI and elevation classes is impossible.

Examining burnt peat plateaus in the same way, elevation class 5 (coefficient = 0.0) and TPI class 4 (coefficient = 0.0) results in a probability of 99 %, however switching TPI to class 1 (coefficient = -5.12) changes the probability to 41 %, which crosses the threshold into "absent" (< 0.5). This anomaly could be attributed to a lack of sampling data representing that unique combination of classes. In the ground-truth data there was only one occurrence of burnt peat plateaus being found on elevation class 5. In this instance its TPI was class 2 (B = 13.1), so there is not a training example of how TPI class 1 would interact with burnt peat plateaus. Thus, in this case this influence is being determined by data points not involving burnt peat plateaus.

Peat plateaus are a similar case where elevation class 5 and TPI class 1 or 4 greatly deviate the probability (0.0 for both). While peat plateaus have the same sampling issues as with burnt peat plateaus although they extend past TPI to elevation. There are no instances of peat plateaus occurring in elevation class 5, this is logical as it would be very rare to have peat plateaus develop in the high areas rather than in the lower elevation classes, due to the lack of organic layer observed in the higher bands (Kuhry, 2008; Zoltai, 1972).

For both peat plateaus and burnt peat plateaus, occurrences in elevation class 5 would be highly unlikely. In the field data one pit recorded as a burnt peat plateau was found in elevation class 5, this might just be an outlier or it could be a misidentification while in the field. In the pit data no occurrences of peat plateaus were found in elevation class five.

It is important to understand the limitations of any model. Micro-climate data was not available for the study area, therefor temperature measurements are not incorporated into this model. This limits our ability to perturb the model for future climate scenarios. If this data were available an approach utilizing these data such as a temperature at the top of permafrost model would be prudent for modelling permafrost temperature in the area (Smith & Riseborough, 2002; Wright et al., 2003).

The TTOP model is a technique which could be used to expand on this work while including climate indices (Riseborough et al., 2008). The TTOP model establishes transfer functions between MAAT, MAGST and TTOP, in specific environments based on their relationship with snow and vegetation cover. With sufficient data a spatial model can be generated and then mapped. The model can then be perturbed to examine future changes in MAAT (Bonnaventure et al., 2017; Garibaldi et al., 2020). A TTOP model is a logical next step and can provide the community with important additional information in planning for permafrost related hazards without using more involved numerical transient models.

While the permafrost probability model produced in this research model provides valuable information about the location of permafrost within a community it does not provide information such as active layer depth, ground ice content, or thermal state of permafrost, therefore it is important to conduct site specific permafrost research before developing.

2.7 Conclusions

As this study only required a single field season and a simple thermal probe to collect data it presents a reasonably simple, labour- and cost-effective way for communities in the boreal discontinuous permafrost zone to better quantify the distribution of permafrost around their community. The results of this model provide considerably more permafrost spatial information at higher resolutions than what has previously been available from regional models. For the community of Whatì this is valuable as the Community Government expects the all-season road, currently under construction, to increase population, land use and development projects in the near future.

The permafrost probability model indicates that 50.0 % of the vegetated area is underlain by permafrost. This model has a statistical accuracy of 91.4 % and an agreement between model values and ground-truth data of 72.8 %.

Whatì can be classified as a "climate driven, ecosystem-modified" permafrost environment. Overlying vegetation was key in modelling permafrost presence. Vegetation classes with undisturbed tree cover as well as thick organic soils and vegetated ground surfaces such as low-shrub organic matter, coniferous forest, peat-plateau and burnt peat-plateau were strong indicators of permafrost. The opposite was the case for classes with near surface mineral soils and more bare ground.

2.8 Acknowledgments

We would like to thank the Community Government of Whatì for their driving role and continued support for the project and acknowledge the Tłı̨chǫ Traditional Territory on which this study took place. Funding for this project was provided by the Climate Change Preparedness

in the North Program. We would also like to thank the Natural Sciences and Engineering Research Council, the University of Lethbridge and the Government of Northwest Territories, Geological Survey for funding contributions and research support. Kochtitzky was supported by the National Science Foundation Graduate Research Fellowship under Grant No. DGE- 1144205 and the Vanier Graduate Scholarship. WorldView imagery and DEMs were provided to Kochtitzky by the Polar Geospatial Center under NSF-OPP awards 1043681, 1559691 and 1542736. We thank Kyle Bexte and Collin Simpson for field assistance, Madeleine Garibaldi for assistance with data and Oliver K. Kienzle for assistance with editing.

2.9 Data Availability Statement

The data that supports the findings is owned by the Community Government of Whatì and managed by the University of Lethbridge. The raw field data is not freely available but will be made available upon reasonable request to the Community Government of Whatì.

Chapter 3

3.1 Conclusions and Future Work

Two objectives were outlined at the beginning of the thesis. Both objectives pertained to examining elements of permafrost mapping in the area around Whatì NT. The first of these objectives was to explore the relationship between permafrost and local environmental variables in order to map the distribution of permafrost in the study area. To achieve this objective a permafrost probability model was created using data obtained from 139 permafrost pits recorded in the field. A high-resolution permafrost probability surface for the community of Whatì was successfully generated from the probability model. The model was informed by ground-truth data recorded over the course of a single field season and yielded accurate and spatially relevant results.

The second objective was to investigate the sensitivity of the local environment and permafrost to change. To explore this objective, the probability surface was modified to reflect different burn scenarios. Landcover classes were separated into burnt and not-burnt variants and used to create permafrost probability models representing scenarios of 100 % burn or 0 % burn in the study area. This process provided an indication of the effect forest fires can have on permafrost in the study area.

The modelling techniques outlined in this thesis have proven to be effective at conducting inexpensive community-based permafrost mapping initiatives. Community-based permafrost mapping was completed for relatively low expense in the community of Whatì. The transferability of this model across different regions and communities has not been evaluated as that would require additional studies which we have not completed. Due to its simplicity, the model would

be easy to modify to model permafrost presence in other communities. However, it is expected that new ground-truth data would be required in order to run a new binary logistic regression model and generate new coefficients. The coefficients generated using the Whatì data may be useable in nearby communities however this has yet to be tested. This would make for an interesting future project.

As mentioned above, testing of this model's transferability would be an interesting project. Nearby communities such as Gamètì and Wekweètì are clear candidates for a study evaluating the transferability of the Whatì model as they are nearby and in similar environments.

The model created in this study is limited as it can only predict current permafrost extent and is not able to be easily perturbed for future climate scenarios. In order to improve permafrost knowledge in the area, a model that is connected to the climate would be more useful. A TTOP model would be ideal as it based off of climate and is therefore able to be perturbed for future climate scenarios, however the model also considers the effect of environmental variables on the connectivity between weather and permafrost.

In order to ensure the creation of a TTOP model for Whatì is possible, seven micro-climate stations and three weather stations were established in the first field season (August 2019). The first complete year of climate data was collected from the micro-climate sensor network in the second field season (September 2020) by myself and another master student at the U of L. This master student will continue the work over the next two years to generate a TTOP model that models the current temperature of the permafrost throughout Whatì as well as the temperature of the permafrost in future climate scenarios.

Snow stakes which will be used to monitor snow depth were also established at 5 of the preexisting sensors, this data will be collected in the third field season (August 2021). At the end

of this second phase of permafrost modelling Whatì will have a high-resolution permafrost probability surface as well as a TTOP model. This will come after only three years of work between two students. This shows that despite low time and resources, high quality modelled surfaces can be created to greatly improve permafrost knowledge of an area. This knowledge will enable the community, regional and territorial governments to inform future development planning and practices to ensure that future developments in permafrost environments are sustainable.

References

Allard, M., Lemay, M., Barrette, C., L'Hérault, E., Sarrazin, D., Bell, T., & Doré, G. (2012). Permafrost and climate change in Nunavik and Nunatsiavut: Importance for municipal and transportation infrastructures. *Nunavik and Nunatsiavut: From science to policy. An Integrated Regional Impact Study (IRIS) of climate change and modernization*, 171-197.

Baral, P., & Haq, M. A. (2020). Spatial prediction of permafrost occurrence in Sikkim Himalayas using logistic regression, random forests, support vector machines and neural networks. *Geomorphology*, 107331.

Bommer, C., Phillips, M., & Arenson, L. U. (2010). Practical recommendations for planning, constructing and maintaining infrastructure in mountain permafrost. *Permafrost and Periglacial Processes, 21*(1), 97-104.

Bonnaventure, P. P., Lamoureux, S. F., & Favaro, E. A. (2017). Over-Winter Channel Bed Temperature Regimes Generated by Contrasting Snow Accumulation in a High Arctic River. *Permafrost and Periglacial Processes, 28*(1), 339-346.

Bonnaventure, P. P., & Lamoureux, S. F. J. P. i. P. G. (2013). The active layer: a conceptual review of monitoring, modelling techniques and changes in a warming climate. *37*(3), 352-376.

Bonnaventure, P. P., & Lewkowicz, A. G. (2008). Mountain permafrost probability mapping using the BTS method in two climatically dissimilar locations, northwest Canada. *Canadian Journal of Earth Sciences, 45*(4), 443-455.

Bonnaventure, P. P., & Lewkowicz, A. G. (2012). Permafrost probability modeling above and below treeline, Yukon, Canada. *Cold Regions Science and Technology, 79*, 92-106.

Bonnaventure, P. P., Lewkowicz, A. G., Kremer, M., & Sawada, M. C. (2012). A permafrost probability model for the southern Yukon and northern British Columbia, Canada. *Permafrost and Periglacial Processes, 23*(1), 52-68.

Brewer, M. C. (1958). Some results of geothermal investigations of permafrost in northern Alaska. *Eos, Transactions American Geophysical Union, 39*(1), 19-26.

Brown, R. (1963). *Influence of vegetation on permafrost, In ed. Wood, K.* Paper presented at the International Conference on Permafrost, Proceedings.

Burn, C., & Friele, P. (1989). Geomorphology, vegetation succession, soil characteristics and permafrost in retrogressive thaw slumps near Mayo, Yukon Territory. *Arctic*, 31-40.

Burn, C. R., & Lewkowicz, A. (1990). Canadian landform examples-17 retrogressive thaw slumps. *Canadian Geographer/Le Géographe canadien, 34*(3), 273-276.

Camill, P., & Clark, J. S. (1998). Climate change disequilibrium of boreal permafrost peatlands caused by local processes. *The American Naturalist, 151*(3), 207-222.

Chasmer, L., Hopkinson, C., Veness, T., Quinton, W., & Baltzer, J. (2014). A decision-tree classification for low-lying complex land cover types within the zone of discontinuous permafrost. *Remote Sensing of Environment, 143*, 73-84.

Connon, R. F., Quinton, W. L., Craig, J. R., & Hayashi, M. (2014). Changing hydrologic connectivity due to permafrost thaw in the lower Liard River valley, NWT, Canada. *Hydrological Processes, 28*(14), 4163-4178.

Cooper, M. D., Estop-Aragonés, C., Fisher, J. P., Thierry, A., Garnett, M. H., Charman, D. J., . . . Kokelj, S. V. (2017). Limited contribution of permafrost carbon to methane release from thawing peatlands. *Nature Climate Change, 7*(7), 507-511.

Côté, M., & Burn, C. (2002). The oriented lakes of Tuktoyaktuk Peninsula, western Arctic coast, Canada: A GIS-based analysis. *Permafrost and Periglacial Processes, 13*(1), 61-70.

Crate, S., Ulrich, M., Habeck, J. O., Desyatkin, A. R., Desyatkin, R. V., Fedorov, A. N., . . . Mészáros, C. (2017). Permafrost livelihoods: A transdisciplinary review and analysis of thermokarst-based systems of indigenous land use. *Anthropocene, 18*, 89-104.

Darrow, M. M., & Jensen, D. D. (2016). Modeling the performance of an air convection embankment (ACE) with thermal berm over ice-rich permafrost, Lost Chicken Creek, Alaska. *Cold Regions Science and Technology, 130*, 43-58.

David W, H., & Stanley, L. (2000). *Apllied Logistic Regression*: Wiley Publishing.

Deluigi, N., Lambiel, C., & Kanevski, M. (2017). Data-driven mapping of the potential mountain permafrost distribution. *Science of The Total Environment, 590*, 370-380.

Doré, G., Niu, F., & Brooks, H. (2016). Adaptation methods for transportation infrastructure built on degrading permafrost. *Permafrost and Periglacial Processes, 27*(4), 352-364.

Etzelmüller, B., Heggem, E. S. F., Sharkhuu, N., Frauenfelder, R., Kääb, A., & Goulden, C. (2006). Mountain permafrost distribution modelling using a multi-criteria approach in the Hövsgöl area, northern Mongolia. *Permafrost and Periglacial Processes, 17*(2), 91-104.

Etzelmüller, B., Hoelzle, M., Flo Heggem, E. S., Isaksen, K., Mittaz, C., Mühll, D. V., . . . Sollid, J. L. (2001). Mapping and modelling the occurrence and distribution of mountain permafrost. *Norsk Geografisk Tidsskrift-Norwegian Journal of Geography, 55*(4), 186-194.

Farbrot, H., Etzelmüller, B., Schuler, T. V., Guðmundsson, Á., Eiken, T., Humlum, O., & Björnsson, H. (2007). Thermal characteristics and impact of climate change on mountain permafrost in Iceland. *Journal of Geophysical Research: Earth Surface, 112*(F3).

Fedorov, A., Konstantinov, P. Y., Vassiliev, I., Bosikov, N., Torgovkin, Y. I., & Samsonova, V. (1998). *Observations of permafrost-landscape dynamics related to anthropogenic disturbances, Yukechi study site, Central Yakutia.* Paper presented at the Permafrost, Seventh International Conference. June 23-27, 1998. Proceedings.

Fisher, D. A., Lacelle, D., & Pollard, W. (2020). A model of unfrozen water content and its transport in icy permafrost soils: Effects on ground ice content and permafrost stability. *Permafrost and Periglacial Processes, 31*(1), 184-199.

Fisher, J. P., Estop-Aragonés, C., Thierry, A., Charman, D. J., Wolfe, S. A., Hartley, I. P., . . . Phoenix, G. K. (2016). The influence of vegetation and soil characteristics on active-layer thickness of permafrost soils in boreal forest. *Global Change Biology, 9*(22), 3127-3140.

Ford, J. D., Cameron, L., Rubis, J., Maillet, M., Nakashima, D., Willox, A. C., & Pearce, T. (2016). Including indigenous knowledge and experience in IPCC assessment reports. *Nature Climate Change, 6*(4), 349-353.

French, H. (2003). The development of periglacial geomorphology: 1-up to 1965. *Permafrost and Periglacial Processes, 14*(1), 29-60.

French, H. (2011). Periglacial environments. *The SAGE handbook of geomorphology. Sage Publications, London*, 393-411.

French, H., & Egginton, P. (1973). *Thermokarst development, Banks Island, western Canadian Arctic.* Paper presented at the 2nd International Conference on Permafrost.

French, H. M., & Williams, P. (1976). *The periglacial environment* (Vol. 341): Wiley Online Library.

Fuentes, D. A., Gamon, J. A., Qiu, H. l., Sims, D. A., & Roberts, D. A. (2001). Mapping Canadian boreal forest vegetation using pigment and water absorption features derived from the AVIRIS sensor. *Journal of Geophysical Research: Atmospheres, 106*(D24), 33565-33577.

Garibaldi, M. C., Bonnaventure, P. P., & Lamoureux, S. F. (2020). Utilizing the TTOP model to understand permafrost temperature variability in High Arctic watershed, Cape Bounty NU.

Genet, H., McGuire, A. D., Barrett, K., Breen, A., Euskirchen, E. S., Johnstone, J., . . . Mack, M. (2013). Modeling the effects of fire severity and climate warming on active layer thickness and soil carbon storage of black spruce forests across the landscape in interior Alaska. *Environmental Research Letters, 8*(4), 045016.

Gibson, C. M., Chasmer, L. E., Thompson, D. K., Quinton, W. L., Flannigan, M. D., & Olefeldt, D. (2018). Wildfire as a major driver of recent permafrost thaw in boreal peatlands. *Nature communications, 9*(1), 1-9.

Goodrich, L. (1982). The influence of snow cover on the ground thermal regime. *Canadian Geotechnical Journal, 19*(4), 421-432.

Gruber, S., & Hoelzle, M. (2001). Statistical modelling of mountain permafrost distribution: local calibration and incorporation of remotely sensed data. *Permafrost and Periglacial Processes, 12*(1), 69-77.

Harris, C., & Lewkowicz, A. G. (2000). An analysis of the stability of thawing slopes, Ellesmere Island, Nunavut, Canada. *Canadian Geotechnical Journal, 37*(2), 449-462.

Harris, S. A. (1981). Climatic relationships of permafrost zones in areas of low winter snow-cover. *Arctic*, 64-70.

Heginbottom, J., Dubreuil, M., & Harker, P. (1995). Canada, Permafrost. National Atlas of Canada. *Natural Resources Canada, 5th Edition, MCR, 4177*.

Henry, K., & Smith, M. (2001). A model-based map of ground temperatures for the permafrost regions of Canada. *Permafrost and Periglacial Processes, 12*(4), 389-398.

Higgins, K. L., & Garon-Labrecque, M. È. (2018). Fine-scale influences on thaw depth in a forested peat plateau landscape in the Northwest Territories, Canada: Vegetation trumps microtopography. *Permafrost and Periglacial Processes, 29*(1), 60-70.

Hinzman, L. D., Goering, D. J., & Kane, D. L. (1998). A distributed thermal model for calculating soil temperature profiles and depth of thaw in permafrost regions. *Journal of Geophysical Research: Atmospheres, 103*(D22), 28975-28991.

Holloway, J. E., & Lewkowicz, A. G. (2020). Half a century of discontinuous permafrost persistence and degradation in western Canada. *Permafrost and Periglacial Processes, 31*(1), 85-96.

Holloway, J. E., Lewkowicz, A. G., Douglas, T. A., Li, X., Turetsky, M. R., Baltzer, J. L., & Jin, H. (2020). Impact of wildfire on permafrost landscapes: A review of recent advances and future prospects. *Permafrost and Periglacial Processes*.

Hosmer, D. W., Lemeshow, S., & Sturdivant, R. X. (2013). *Applied logistic regression* (Vol. 398): John Wiley & Sons.

Hovelsrud, G. K., & Smit, B. (2010). *Community adaptation and vulnerability in Arctic regions*: Springer.

Hu, G., Zhao, L., Wu, X., Li, R., Wu, T., Xie, C., . . . Zou, D. (2017). Comparison of the thermal conductivity parameterizations for a freeze-thaw algorithm with a multi-layered soil in permafrost regions. *Catena, 156*, 244-251.

Jafarov, E. E., Coon, E. T., Harp, D. R., Wilson, C. J., Painter, S. L., Atchley, A. L., & Romanovsky, V. E. (2018). Modeling the role of preferential snow accumulation in through talik development and hillslope groundwater flow in a transitional permafrost landscape. *Environmental Research Letters, 13*(10), 105006.

Jafarov, E. E., Romanovsky, V. E., Genet, H., McGuire, A. D., & Marchenko, S. S. (2013). The effects of fire on the thermal stability of permafrost in lowland and upland black spruce forests of interior Alaska in a changing climate. *Environmental Research Letters, 8*(3), 035030.

Jiang, Y., Rocha, A. V., O'Donnell, J. A., Drysdale, J. A., Rastetter, E. B., Shaver, G. R., & Zhuang, Q. (2015). Contrasting soil thermal responses to fire in Alaskan tundra and boreal forest. *Journal of Geophysical Research: Earth Surface, 120*(2), 363-378.

Jin, H.-j., Yu, Q.-h., Wang, S.-l., & Lü, L.-z. (2008). Changes in permafrost environments along the Qinghai–Tibet engineering corridor induced by anthropogenic activities and climate warming. *Cold Regions Science and Technology, 53*(3), 317-333.

Jorgenson, M. T., & Grosse, G. (2016). Remote sensing of landscape change in permafrost regions. *Permafrost and Periglacial Processes, 27*(4), 324-338.

Jorgenson, M. T., Harden, J., Kanevskiy, M., O'Donnell, J., Wickland, K., Ewing, S., . . . Striegl, R. (2013). Reorganization of vegetation, hydrology and soil carbon after permafrost degradation across heterogeneous boreal landscapes. *Environmental Research Letters, 8*(3), 035017.

Jorgenson, M. T., Romanovsky, V., Harden, J., Shur, Y., O'Donnell, J., Schuur, E. A., . . . Marchenko, S. (2010). Resilience and vulnerability of permafrost to climate change. *Canadian Journal of Forest Research, 40*(7), 1219-1236.

Kääb, A. (2008). Remote sensing of permafrost-related problems and hazards. *Permafrost and Periglacial Processes, 19*(2), 107-136.

Karunaratne, K., & Burn, C. (2003). *Freezing n-factors in discontinuous permafrost terrain, Takhini River, Yukon Territory, Canada.* Paper presented at the Proceedings of the 8th International Conference on Permafrost, July.

Kasischke, E. S., & Stocks, B. J. (2012). *Fire, climate change, and carbon cycling in the boreal forest* (Vol. 138): Springer Science & Business Media.

Kasischke, E. S., Verbyla, D. L., Rupp, T. S., McGuire, A. D., Murphy, K. A., Jandt, R., . . . Calef, M. (2010). Alaska's changing fire regime—implications for the vulnerability of its boreal forests. *Canadian Journal of Forest Research, 40*(7), 1313-1324.

Klene, A. E., Nelson, F. E., Shiklomanov, N. I., & Hinkel, K. M. (2001). The n-factor in natural landscapes: variability of air and soil-surface temperatures, Kuparuk River Basin, Alaska, USA. *Arctic, Antarctic, and Alpine Research, 33*(2), 140-148.

Kokelj, S., Tunnicliffe, J., Lacelle, D., Lantz, T., Chin, K., & Fraser, R. (2015). Increased precipitation drives mega slump development and destabilization of ice-rich permafrost terrain, northwestern Canada. *Global and Planetary Change, 129*, 56-68.

Kokelj, S. V., Lantz, T. C., Tunnicliffe, J., Segal, R., & Lacelle, D. (2017). Climate-driven thaw of permafrost preserved glacial landscapes, northwestern Canada. *Geology, 45*(4), 371-374.

Korpela, I., Koskinen, M., Vasander, H., Holopainen, M., & Minkkinen, K. (2009). Airborne small-footprint discrete-return LiDAR data in the assessment of boreal mire surface patterns, vegetation, and habitats. *Forest ecology and management, 258*(7), 1549-1566.

Kremer, M., Lewkowicz, A. G., Bonnaventure, P. P., & Sawada, M. C. (2011). Utility of classification and regression tree analyses and vegetation in mountain permafrost models, Yukon, Canada. *Permafrost and Periglacial Processes, 22*(2), 163-178.

Krupnik, I., & Jolly, D. (2002). *The Earth Is Faster Now: Indigenous Observations of Arctic Environmental Change. Frontiers in Polar Social Science*: ERIC.

Kuhry, P. (2008). Palsa and peat plateau development in the Hudson Bay Lowlands, Canada: timing, pathways and causes. *Boreas, 37*(2), 316-327.

Lachenbruch, A. H. (1994). *Permafrost, the active layer, and changing climate*: Citeseer.

Laing, J., & Binyamin, J. (2013). Climate change effect on winter temperature and precipitation of Yellowknife, Northwest Territories, Canada from 1943 to 2011. *American Journal of Climate Change, 2013*.

Larsen, P. F., Phinney, D. A., Rubin, F., & Justice, D. (2009). Classification of boreal macrotidal littoral zone habitats in the Gulf of Maine: comparison of IKONOS and CASI multispectral imagery. *Geocarto International, 24*(6), 457-472.

Legendre, M., Lartigue, A., Bertaux, L., Jeudy, S., Bartoli, J., Lescot, M., . . . Labadie, K. (2015). In-depth study of Mollivirus sibericum, a new 30,000-y-old giant virus infecting Acanthamoeba. *Proceedings of the National Academy of Sciences, 112*(38), E5327-E5335.

Lewkowicz, A. G. (2007). Dynamics of active-layer detachment failures, Fosheim peninsula, Ellesmere Island, Nunavut, Canada. *Permafrost and Periglacial Processes, 18*(1), 89-103.

Lewkowicz, A. G., & Bonnaventure, P. P. (2008). Interchangeability of mountain permafrost probability models, northwest Canada. *Permafrost and Periglacial Processes, 19*(1), 49-62.

Lewkowicz, A. G., & Coultish, T. L. (2004). Beaver damming and palsa dynamics in a subarctic mountainous environment, Wolf Creek, Yukon Territory, Canada. *Arctic, Antarctic, and Alpine Research, 36*(2), 208-218.

Lewkowicz, A. G., & Ednie, M. (2004). Probability mapping of mountain permafrost using the BTS method, Wolf Creek, Yukon Territory, Canada. *Permafrost and Periglacial Processes, 15*(1), 67-80.

Ling, F., & Zhang, T. (2004). A numerical model for surface energy balance and thermal regime of the active layer and permafrost containing unfrozen water. *Cold Regions Science and Technology, 38*(1), 1-15.

Lunardini, V. J. (1978). *Theory of n-factors and correlation of data.* Paper presented at the Proceedings of the Third International Conference on Permafrost.

Lunardini, V. J. (1981). *Heat transfer in cold climates*: Van Nostrand Reinhold Company.

Luo, J., Niu, F., Lin, Z., Liu, M., & Yin, G. (2019). Recent acceleration of thaw slumping in permafrost terrain of Qinghai-Tibet Plateau: An example from the Beiluhe Region. *Geomorphology, 341*, 79-85.

Ma, T., Tang, T., Ding, X., Huang, X., & Zhao, Y. (2018). Thermal Regime Analysis and Protective Measure Evaluation for Wide Embankment in Permafrost Regions of Qinghai-Tibet Plateau. *International Journal of Civil Engineering, 16*(10), 1303-1316.

MacDougall, A. H., Avis, C. A., & Weaver, A. J. (2012). Significant contribution to climate warming from the permafrost carbon feedback. *Nature Geoscience, 5*(10), 719-721.

Mackay, J. R. (1970). Disturbances to the tundra and forest tundra environment of the western Arctic. *Canadian Geotechnical Journal, 7*(4), 420-432.

Michalowski, R. L., & Zhu, M. (2006). Frost heave modelling using porosity rate function. *International journal for numerical and analytical methods in geomechanics, 30*(8), 703-722.

Morsdorf, F., Meier, E., Kötz, B., Itten, K. I., Dobbertin, M., & Allgöwer, B. (2004). LIDAR-based geometric reconstruction of boreal type forest stands at single tree level for forest and wildland fire management. *Remote Sensing of Environment, 92*(3), 353-362.

Myers-Smith, I., Harden, J., Wilmking, M., Fuller, C., McGuire, A., & FS III, C. (2008). Wetland succession in a permafrost collapse: interations between fire and thermokarst. *Biogeosciences. 5: 1273-1286*.

Nagelkerke, N. J. (1991). A note on a general definition of the coefficient of determination. *Biometrika, 78*(3), 691-692.

Nelson, F. E. (2003). (Un) frozen in time. *Science, 299*(5613), 1673-1675.

Nixon, F. M., & Taylor, A. E. (1998). *Regional active layer monitoring across the sporadic, discontinuous and continuous permafrost zones, Mackenzie Valley, northwestern Canada.* Paper presented at the Proceedings of the Seventh International Conference on Permafrost.

Noh, M.-J., & Howat, I. M. (2017). The surface extraction from TIN based search-space minimization (SETSM) algorithm. *ISPRS Journal of Photogrammetry and Remote Sensing, 129*, 55-76.

Obu, J., Westermann, S., Bartsch, A., Berdnikov, N., Christiansen, H. H., Dashtseren, A., . . . Kholodov, A. (2019). Northern Hemisphere permafrost map based on TTOP modelling for 2000–2016 at 1 km2 scale. *Earth-Science Reviews*.

Oreskes, N., Shrader-Frechette, K., & Belitz, K. (1994). Verification, validation, and confirmation of numerical models in the earth sciences. *Science, 263*(5147), 641-646.

Osterkamp, T., Jorgenson, M., Schuur, E., Shur, Y., Kanevskiy, M., Vogel, J., & Tumskoy, V. (2009). Physical and ecological changes associated with warming permafrost and thermokarst in interior Alaska. *Permafrost and Periglacial Processes, 20*(3), 235-256.

Painter, S. L., Moulton, J. D., & Wilson, C. (2013). Modeling challenges for predicting hydrologic response to degrading permafrost. *Hydrogeology Journal, 21*(1), 221-224.

Panda, S. K., Prakash, A., Solie, D. N., Romanovsky, V. E., & Jorgenson, M. T. (2010). Remote sensing and field-based mapping of permafrost distribution along the Alaska Highway corridor, interior Alaska. *Permafrost and Periglacial Processes, 21*(3), 271-281.

Paramonov, V., Sakharov, I., & Kudriavtcev, S. (2016). *Forecast the processes of thawing of permafrost soils under the building with the large heat emission.* Paper presented at the MATEC web of conferences.

Pastick, N. J., Jorgenson, M. T., Wylie, B. K., Rose, J. R., Rigge, M., & Walvoord, M. A. (2014). Spatial variability and landscape controls of near-surface permafrost within the Alaskan Yukon River Basin. *Journal of Geophysical Research: Biogeosciences, 119*(6), 1244-1265.

Peel, M. C., Finlayson, B. L., & McMahon, T. A. (2007). Updated world map of the Köppen-Geiger climate classification.

Penner, E., & Goodrich, L. (1982). Location of segregated ice in frost-susceptible soil. In *Developments in Geotechnical Engineering* (Vol. 28, pp. 231-244): Elsevier.

Perreault, P., & Shur, Y. (2016). Seasonal thermal insulation to mitigate climate change impacts on foundations in permafrost regions. *Cold Regions Science and Technology, 132*, 7-18.

Porada, P., Ekici, A., & Beer, C. (2016). Effects of bryophyte and lichen cover on permafrost soil temperature at large scale. *The Cryosphere, 10*(5), 2291.

Price, J. C. (1981). The contribution of thermal data in Landsat multispectral classification. *Photogrammetric Engineering and Remote Sensing, 47*(2), 229-236.

Quinton, W., Berg, A., Braverman, M., Carpino, O., Chasmer, L., Connon, R., . . . Haynes, K. (2019). A synthesis of three decades of hydrological research at Scotty Creek, NWT, Canada. *Hydrology & Earth System Sciences, 23*(4).

Quinton, W., Hayashi, M., & Chasmer, L. (2011). Permafrost-thaw-induced land-cover change in the Canadian subarctic: implications for water resources. *Hydrological Processes, 25*(1), 152-158.

Regmi, P., Grosse, G., Jones, M. C., Jones, B. M., & Anthony, K. W. (2012). Characterizing post-drainage succession in thermokarst lake basins on the Seward Peninsula, Alaska with TerraSAR-X backscatter and Landsat-based NDVI data. *Remote Sensing, 4*(12), 3741-3765.

Riseborough, D., Shiklomanov, N., Etzelmüller, B., Gruber, S., & Marchenko, S. (2008). Recent advances in permafrost modelling. *Permafrost and Periglacial Processes, 19*(2), 137-156.

Romanovsky, V., & Osterkamp, T. (1995). Interannual variations of the thermal regime of the active layer and near-surface permafrost in northern Alaska. *Permafrost and Periglacial Processes, 6*(4), 313-335.

Romanovsky, V. E., & Osterkamp, T. (2000). Effects of unfrozen water on heat and mass transport processes in the active layer and permafrost. *Permafrost and Periglacial Processes, 11*(3), 219-239.

Schuster, P. F., Schaefer, K. M., Aiken, G. R., Antweiler, R. C., Dewild, J. F., Gryziec, J. D., . . . Krabbenhoft, D. P. (2018). Permafrost stores a globally significant amount of mercury. *Geophysical Research Letters, 45*(3), 1463-1471.

Schuur, E. A., McGuire, A. D., Schädel, C., Grosse, G., Harden, J., Hayes, D. J., . . . Lawrence, D. M. (2015). Climate change and the permafrost carbon feedback. *Nature, 520*(7546), 171-179.

Shur, Y., & Jorgenson, M. (2007). Patterns of permafrost formation and degradation in relation to climate and ecosystems. *Permafrost and Periglacial Processes, 18*(1), 7-19.

Smith, M. (1990). Potential responses of permafrost to climatic change. *Journal of cold regions engineering, 4*(1), 29-37.

Smith, M., & Riseborough, D. (1996). Permafrost monitoring and detection of climate change. *Permafrost and Periglacial Processes, 7*(4), 301-309.

Smith, M., & Riseborough, D. (2002). Climate and the limits of permafrost: a zonal analysis. *Permafrost and Periglacial Processes, 13*(1), 1-15.

Smith, S. L., & Riseborough, D. W. (2010). Modelling the thermal response of permafrost terrain to right-of-way disturbance and climate warming. *Cold Regions Science and Technology, 60*(1), 92-103.

Smith, S. L., Riseborough, D. W., & Bonnaventure, P. P. (2015). Eighteen year record of forest fire effects on ground thermal regimes and permafrost in the Central Mackenzie Valley, NWT, Canada. *Permafrost and Periglacial Processes, 26*(4), 289-303.

Tarasenko, A., Redutinskiy, M., Chepur, P., & Gruchenkova, A. (2018). *Study of stress-strain state of pipeline under permafrost conditions*. Paper presented at the Journal of Physics: Conference Series.

Taylor, A. E., Dallimore, S., Hill, P., Issler, D., Blasco, S., & Wright, F. (2013). Numerical model of the geothermal regime on the Beaufort Shelf, arctic Canada since the Last Interglacial. *Journal of Geophysical Research: Earth Surface, 118*(4), 2365-2379.

Thomas, H. R., Cleall, P., Li, Y.-C., Harris, C., & Kern-Luetschg, M. (2009). Modelling of cryogenic processes in permafrost and seasonally frozen soils. *Geotechnique, 59*(3), 173-184.

Tucker, C., & Sellers, P. (1986). Satellite remote sensing of primary production. *International Journal of Remote Sensing, 7*(11), 1395-1416.

Turetsky, M., Donahue, W., & Benscoter, B. (2011). Experimental drying intensifies burning and carbon losses in a northern peatland. *Nature communications, 2*(1), 1-5.

Turetsky, M. R., Mack, M. C., Hollingsworth, T. N., & Harden, J. W. (2010). The role of mosses in ecosystem succession and function in Alaska's boreal forest. *Canadian Journal of Forest Research, 40*(7), 1237-1264.

Van Vliet-Lanoë, B. (1985). Frost effects in soils. *Soils and quaternary landscape evolution*, 117-158.

Walker, J., Arnborg, L., & Peippo, J. (1987). Riverbank erosion in the Colville delta, Alaska. *Geografiska Annaler: Series A, Physical Geography, 69*(1), 61-70.

AdaptWest Project. Gridded current and projected climate data for North America at 1 km resolution, interpolated using the *ClimateNA v5. 10* software (T. Wang et al., 2015). Available at adaptwest.databasin.org.

Wang, T., Hamann, A., Spittlehouse, D., & Carroll, C. (2016). Locally downscaled and spatially customizable climate data for historical and future periods for North America. *PloS one, 11*(6), e0156720.

Wang, X., Thompson, D. K., Marshall, G. A., Tymstra, C., Carr, R., & Flannigan, M. D. (2015). Increasing frequency of extreme fire weather in Canada with climate change. *Climatic Change, 130*(4), 573-586.

Way, R. G., & Lewkowicz, A. G. (2016). Modelling the spatial distribution of permafrost in Labrador–Ungava using the temperature at the top of permafrost. *Canadian Journal of Earth Sciences, 53*(10), 1010-1028.

Way, R. G., & Lewkowicz, A. G. (2018). Environmental controls on ground temperature and permafrost in Labrador, northeast Canada. *Permafrost and Periglacial Processes, 29*(2), 73-85.

Wellman, T. P., Voss, C. I., & Walvoord, M. A. (2013). Impacts of climate, lake size, and supra-and sub-permafrost groundwater flow on lake-talik evolution, Yukon Flats, Alaska (USA). *Hydrogeology Journal, 21*(1), 281-298.

Wolfe, S. A. (1998). *Living with frozen ground: a field guide to permafrost in Yellowknife, Northwest Territories* (Vol. 64): Geological Survey of Canada.

Wright, J., Duchesne, C., & Côté, M. (2003). *Regional-scale permafrost mapping using the TTOP ground temperature model*. Paper presented at the Proceedings 8th International Conference on Permafrost. Swets and Zeitlinger, Lisse.

Yang, D., & Woo, M. K. (1999). Representativeness of local snow data for large scale hydrologic investigations. *Hydrological Processes, 13*(12-13), 1977-1988.

Yi, S., McGuire, A. D., Kasischke, E., Harden, J., Manies, K., Mack, M., & Turetsky, M. (2010). A dynamic organic soil biogeochemical model for simulating the effects of wildfire on soil environmental conditions and carbon dynamics of black spruce forests. *Journal of Geophysical Research: Biogeosciences, 115*(G4).

Yi, S., Woo, M. k., & Arain, M. A. (2007). Impacts of peat and vegetation on permafrost degradation under climate warming. *Geophysical Research Letters, 34*(16).

Yoshikawa, K., Bolton, W. R., Romanovsky, V. E., Fukuda, M., & Hinzman, L. D. (2002). Impacts of wildfire on the permafrost in the boreal forests of Interior Alaska. *Journal of Geophysical Research: Atmospheres, 107*(D1), FFR 4-1-FFR 4-14.

Zhang, T. (2005). Influence of the seasonal snow cover on the ground thermal regime: An overview. *Reviews of Geophysics, 43*(4).

Zhang, T., Barry, R. G., & Haeberli, W. (2001). Numerical simulations of the influence of the seasonal snow cover on the occurrence of permafrost at high latitudes. *Norsk Geografisk Tidsskrift-Norwegian Journal of Geography, 55*(4), 261-266.

Zhang, Y., Chen, W., & Riseborough, D. W. (2008). Disequilibrium response of permafrost thaw to climate warming in Canada over 1850–2100. *Geophysical Research Letters, 35*(2).

Zhang, Y., Wolfe, S. A., Morse, P. D., Olthof, I., & Fraser, R. H. (2015). Spatiotemporal impacts of wildfire and climate warming on permafrost across a subarctic region, Canada. *Journal of Geophysical Research: Earth Surface, 120*(11), 2338-2356.

Zhao, S., Cheng, W., Zhou, C., Chen, X., & Chen, J. (2012). Simulation of decadal alpine permafrost distributions in the Qilian Mountains over past 50 years by using Logistic Regression Model. *Cold Regions Science and Technology, 73*, 32-40.

Zheng, H., Kanie, S., & Niu, F. (2018). The thermal regime evaluation of high-speed railway foundation by mixed hybrid FEM. *Cold Regions Science and Technology, 155*, 333-342.

Zhuang, Q., Romanovsky, V., & McGuire, A. (2001). Incorporation of a permafrost model into a large-scale ecosystem model: Evaluation of temporal and spatial scaling issues in simulating soil thermal dynamics. *Journal of Geophysical Research: Atmospheres, 106*(D24), 33649-33670.

Zoltai, S. (1972). Palsas and peat plateaus in central Manitoba and Saskatchewan. *Canadian Journal of Forest Research, 2*(3), 291-302.